Bleb-driven chemotaxis of *Dictyostelium* cells

Evgeny Zatulovskiy,[1] Richard Tyson,[2] Till Bretschneider,[2] and Robert R. Kay[1]

[1]MRC Laboratory of Molecular Biology, Cambridge CB2 0QH, England, UK
[2]Warwick Systems Biology Centre, University of Warwick, Coventry CV4 7AL, England, UK

Blebs and F-actin–driven pseudopods are alternative ways of extending the leading edge of migrating cells. We show that *Dictyostelium* cells switch from using predominantly pseudopods to blebs when migrating under agarose overlays of increasing stiffness. Blebs expand faster than pseudopods leaving behind F-actin scars, but are less persistent. Blebbing cells are strongly chemotactic to cyclic-AMP, producing nearly all of their blebs up-gradient. When cells re-orientate to a needle releasing cyclic-AMP, they stereotypically produce first microspikes, then blebs and pseudopods only later. Genetically, blebbing requires myosin-II and increases when actin polymerization or cortical function is impaired. Cyclic-AMP induces transient blebbing independently of much of the known chemotactic signal transduction machinery, but involving PI3-kinase and downstream PH domain proteins, CRAC and PhdA. Impairment of this PI3-kinase pathway results in slow movement under agarose and cells that produce few blebs, though actin polymerization appears unaffected. We propose that mechanical resistance induces bleb-driven movement in *Dictyostelium*, which is chemotactic and controlled through PI3-kinase.

Introduction

Motile cells can vary greatly in shape, speed, and ability to move in different environments, but are powered by a limited number of conserved processes. Central among these is extension of the leading edge (Insall and Machesky, 2009; Lämmermann and Sixt, 2009). Crawling cells, including fibroblasts, neutrophils, and *Dictyostelium* amoebae, usually extend their leading edge by actin polymerization (Pollard and Borisy, 2003): F-actin filaments grow and branch beneath the plasma membrane as a dendritic network (Svitkina and Borisy, 1999), applying force to the membrane and thus extending it (Mogilner and Oster, 1996).

Alternatively, certain cells can extend their leading edge using blebs (Charras and Paluch, 2008). Blebs are smooth, rounded projections of the plasma membrane formed when it separates from the underlying actin cortex and is driven out by fluid pressure. This pressure is provided by contraction of the cell cortex, and there is little if any F-actin beneath the bleb membrane as it expands (Charras et al., 2008). Bleb-driven motility is unusual in cells moving under buffer on a planar surface, but can be prominent in three-dimensional environments, including within the tissues of developing embryos (Trinkaus, 1973; Sahai and Marshall, 2003; Wolf et al., 2003; Blaser et al., 2006; Diz-Muñoz et al., 2010; Otto et al., 2011).

Cancer cells among others can be quite flexible in how they move, switching between F-actin–driven and bleb- or pressure-driven motility according to their environment (Trinkaus et al., 1992; Sahai and Marshall, 2003; Wolf et al., 2003; Petrie et al., 2012; Tozluoğlu et al., 2013) and being able to compensate for genetic impairment of dendritic actin polymerization by using unbranched actin filaments or blebs to move instead (Derivery et al., 2008; Suraneni et al., 2012; Wu et al., 2012). This flexibility may assist cells in moving within complicated three-dimensional environments, but raises the question of what physical and chemical features of the environment are sensed by cells to control their migration mode.

Many motile cells are chemotactic (Kay et al., 2008; Insall, 2010; Swaney et al., 2010). One view holds that they orientate by comparing chemoattractant concentrations globally to produce a localized internal signal—a chemotactic compass—that determines where pseudopods form, and hence the direction of movement (Xiong et al., 2010). Alternatively, chemotaxis might be mediated by more local interactions (Arrieumerlou and Meyer, 2005) or by competition between existing pseudopods (Insall, 2010). Whatever the molecular mechanism of chemotactic orientation, it is widely assumed that the ultimate target is some aspect of actin dynamics. Bleb-driven cells are also likely to be chemotactic (Fink and Trinkaus, 1988; Blaser et al., 2006), raising

Correspondence to Robert R. Kay: rrk@mrc-lmb.cam.ac.uk

The Rockefeller University Press $30.00
J. Cell Biol. Vol. 204 No. 6 1027–1044
www.jcb.org/cgi/doi/10.1083/jcb.201306147

the question of how chemotactic signals determine where blebs will form.

Dictyostelium cells, with their rapid movement and powerful molecular genetics, have become a standard system to investigate basic aspects of cell motility (King and Insall, 2009; Swaney et al., 2010). Chemotaxis is usually studied at a transitional phase in development, in which separate cells aggregate together by chemotaxis to cyclic-AMP, en route to forming multicellular structures. Thus, these cells make a natural transition from moving separately on a planar surface to moving within the mechanically resistive, three-dimensional confines of a tissue.

Dictyostelium cells are generally thought to move under buffer using actin-driven pseudopods, but a single report also describes them as using small, transient blebs as well as pseudopods (Yoshida and Soldati, 2006), and uniform stimulation with cyclic-AMP can induce blebbing, suggesting that blebs are under chemotactic control (Langridge and Kay, 2006). In this work we show that pure bleb-driven movement can be evoked by mechanical resistance, and is strongly chemotactic. A genetic screen suggests that blebbing in response to chemoattractant is controlled through PI3-kinase and two downstream PIP3-binding proteins.

Results

Blebbing is a standard part of *Dictyostelium* cell motility

Blebbing was previously reported at the leading edge when cells of one particular *Dictyostelium* strain migrated under buffer (Yoshida and Soldati, 2006). Because laboratory strains can differ significantly in genetic background and phenotype (Pollitt et al., 2006; Bloomfield et al., 2008), we first generalized this observation using aggregation-competent cells (cells starved for 5–6 h, and chemotactic to cyclic-AMP). We found that blebs, as well as F-actin–driven pseudopods, are readily apparent at the leading edge of a range of genetically distinct strains, including the wild isolate, NC4, the historically important DdB, our laboratory working stock of Ax2 (Fig. 1 and Video 1) and a set of parental strains from other laboratories tested in our genetic screen for blebbing mutants (see Table S1).

Blebs are recognized by three main characteristics: they are rounded and smooth without any granular contents visible under DIC; they expand very rapidly, typically in less than one second (see Fig. 4); and they leave behind an F-actin "scar," representing the former position of the cortex, which can be visualized with F-actin reporters such as ABD-GFP or LifeAct (Pang et al., 1998; Riedl et al., 2008; Figs. 1 and 2; see Videos 1, 4, and 5). The F-actin scar is short-lived, disappearing in a few seconds, and at the same time a new cortex builds beneath the membrane of the bleb, so that the whole life-cycle of a bleb is completed in less than 10 seconds. Because this is less than the frame-rate of many chemotaxis movies, it may account—along with their small size—for why blebs have often been overlooked in studies of *Dictyostelium* chemotaxis.

Blebs and F-actin–driven protrusions can coexist at the leading edge in various ways. Blebs can transform into actin-driven structures by continued actin polymerization at the cortex (Fig. 1, C and E), and actin-driven processes can spawn blebs at their margins. This often results in hybrid structures containing multiple blebs and areas of actin polymerization, all stabilized by an F-actin framework (Fig. 1, D and E; and Video 2, "blebbopodia").

We noticed that blebbing is developmentally regulated. Blebs are rare in growing cells during random movement, but increase nearly 10-fold in frequency by 8 h of development, to around 4 blebs per cell, per minute (Fig. 3 A). Blebs formed in response to a cyclic-AMP shock (see Materials and methods) increased in a similar fashion. By the time multicellular streams form, bleb-driven motility is the norm for the cells leading small streams, which have an unrestricted leading edge (Fig. 1 B and Video 3).

Increased mechanical resistance induces bleb-driven motility

Blebbing motility is most commonly observed in vertebrate cells as they migrate through solid tissues or in a three-dimensional matrix, and in *Dictyostelium* blebbing increases as cells prepare for multicellular development. A common factor linking these observations is that in each case the cells move (or are preparing to move) against increased mechanical resistance. This suggests that mechanical resistance alone might be sufficient to induce blebbing motility.

To test this hypothesis, we induced *Dictyostelium* cells to move under agarose overlays of increasing strength and hence increasing mechanical resistance (Fig. 3 D). The cells were placed in a well in the agarose, and attracted to move under it, toward another well containing cyclic-AMP (Laevsky and Knecht, 2001). The effect of the overlay is clear-cut (Fig. 2, Fig. 3 B, and Video 4): the proportion of blebs compared with total cellular projections increases from 20 to 30% under buffer, to approaching 100% in the same cells moving under overlays of more than 1% agarose (Young's modulus 70–80 kPa; Fig. 3 D). An F-actin reporter shows that blebs leave behind F-actin scars at the site of the former cortex and that the newly expanded membrane is almost devoid of F-actin, but regains an F-actin cortex within a second (Fig. 2, A and B), similar to cells moving under buffer.

We considered various features of the under-agarose set up that might account for the increased blebbing. Confocal microscopy showed that cells continue to move on the surface of the coverslip once under agarose, but became flattened in proportion to the strength of the agarose (Fig. 3 C and Video 5 Laevsky and Knecht, 2001; Traynor and Kay, 2007). In a control experiment, we found that cells embedded directly in agarose are not flattened but still bleb copiously (Fig. 2 C). These embedded cells move less well than on glass, presumably because they cannot gain good traction. We tested whether the chemical nature of the overlay is critical and found that cells moving on top of agarose did not switch to blebbing, whereas those under a layer of washed 8% polyacrylamide gel blebbed strongly (not depicted). We also observed that blebbing increased in vegetative cells when they are attracted under agarose by a gradient of folic acid (not depicted). These experiments show that the switch to bleb-driven movement under agarose is not due to a change in substratum, cell flattening, the chemical nature of the overlay, or the particular chemoattractant used.

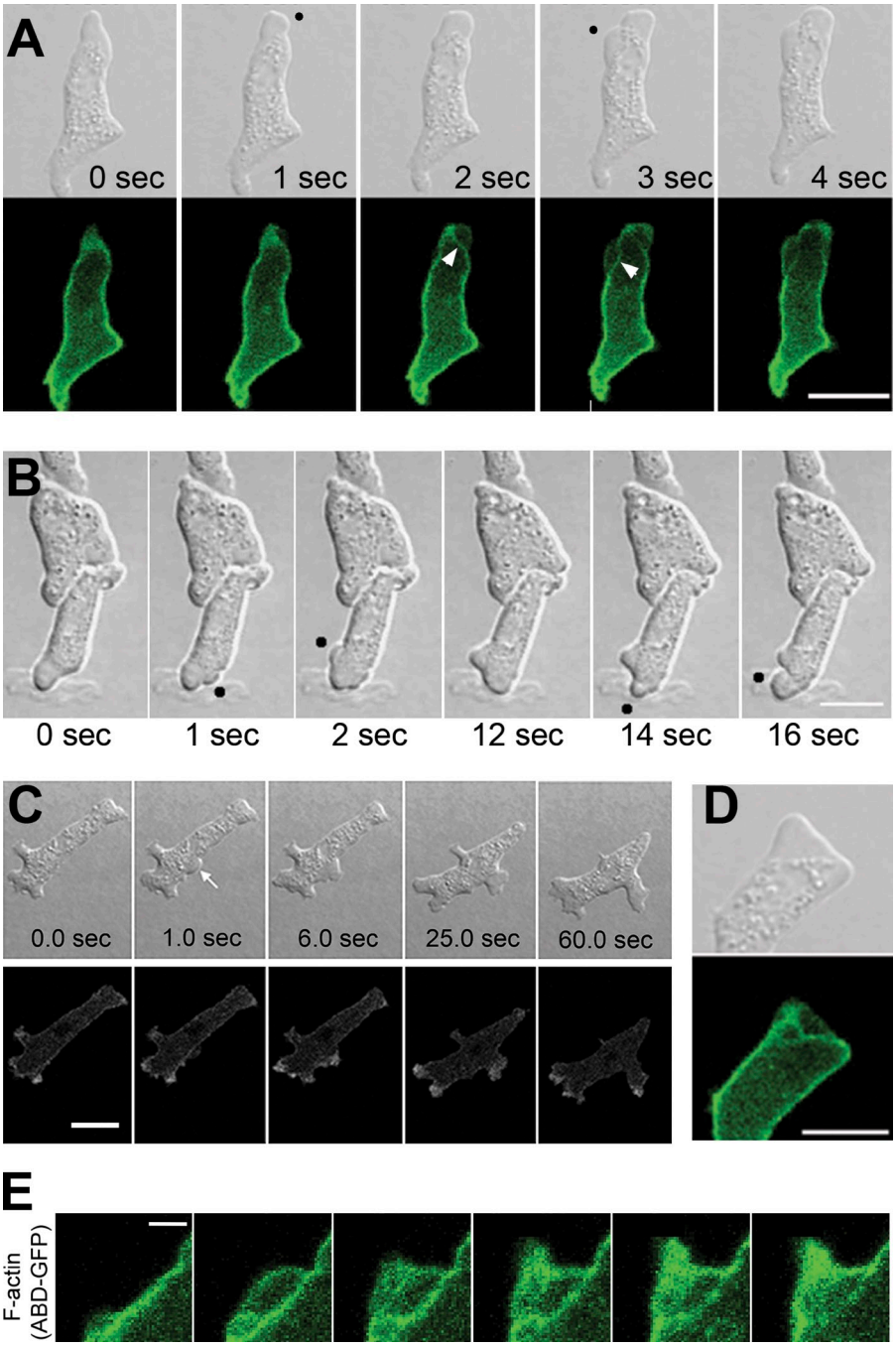

Figure 1. **Blebs formed by *Dictyostelium* cells moving under buffer.** (A) Blebs (black dots) formed at the leading edge of a cell expressing an F-actin reporter. Blebs are small and expand in less than one second, leaving behind an F-actin scar (white arrows), but rapidly regain an F-actin cortex (see Video 1). (B) The cell leading a small stream moving in bleb mode (see Video 3). (C) Transformation of a bleb (arrowed) into a pseudopod by continued actin polymerization. (D) A composite bleb and pseudopod ("blebbopodium"). (E) Detail of the transformation of a bleb into a pseudopod by continued actin polymerization (see Video 2). Ax2 cells expressing the F-actin reporter ABD120-GFP were starved for 5.5 h, or 6.5 h for B. Confocal fluorescence and DIC images obtained at 1 frame per second; Bars: (A, B, and D) 10 µm; (E) 1 µm.

The pore diameter of agarose—0.5 µm for 1% agarose (Maaloum et al., 1998)—is much smaller than the cell diameter and we do not see any evidence from movies or 3D reconstructions that cells snake through pores in the agarose, as tumor cells can through the much larger pores of collagen gels (Wolf et al., 2013). Small (0.45-µm diameter) fluorescent beads were incorporated into the agarose to track its movement as the cells passed beneath (Video 5, final section). Typically, the beads move just before a cell reaches them and are restored to their original position once it has passed, as evidenced by the changes in fluorescence as the beads move into and out of the confocal section (Laevsky and Knecht, 2001). This deformation of the agarose by the passing cells demonstrates that they exert mechanical force on the agarose and conversely, must experience mechanical resistance from it.

It therefore appears that cells moving under agarose experience a continuous, fine-grained, resistive matrix, which they cannot infiltrate, but must deform if they are to pass. The simplest explanation for our observations is that mechanical resistance from this matrix is sufficient to switch cells to bleb-driven motility, with mechanical resistance here defined as the force cells exert to deform the matrix.

Analysis of bleb and pseudopod dynamics

Cells expressing the F-actin reporter ABD-GFP were filmed at 2–6 Hz under 0.7% agarose, and their outlines revealed by

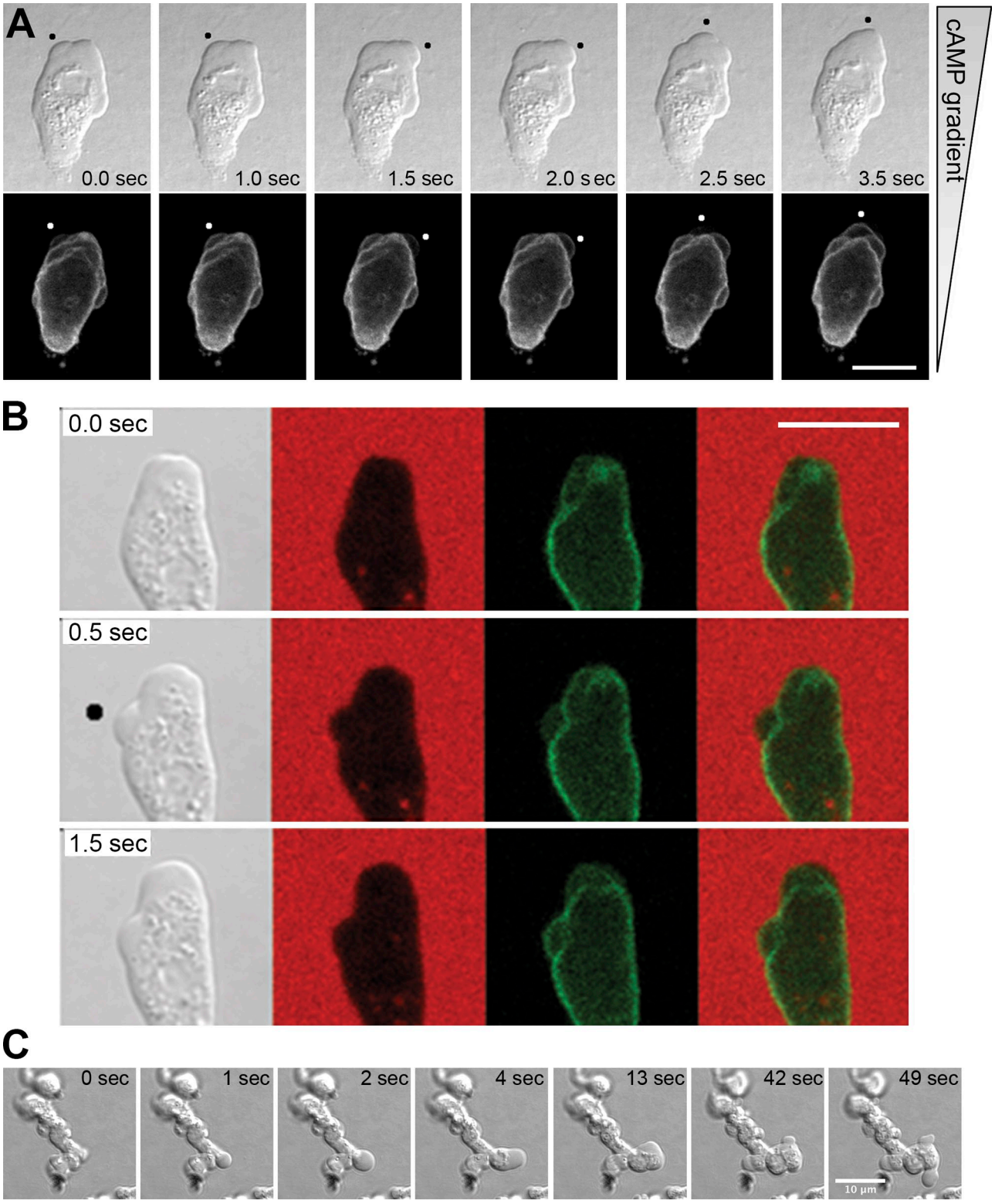

Figure 2. **Bleb-driven movement is induced by mechanical resistance.** (A) Mechanical resistance provided by an overlay of 0.7% agarose induces a cell to move entirely in bleb mode. Blebs (dots) leave behind their cortical F-actin as a scar when they expand (see Video 4). (B) Blebs produced by a cell moving under a 0.7% agarose overlay containing fluorescent dye (0.5 mg/ml RITC-dextran) to reveal its outline. A bleb (dot) expands in less than 0.5 s, leaving behind an F-actin scar; it initially lacks an F-actin cortex, but rebuilds one in another second (see Video 6). (C) Cells embedded in 0.5% low melting-point agarose produce copious blebs. Ax2 cells used throughout, and expressing the F-actin reporter ABD-GFP in A and B. Bar, 10 µm.

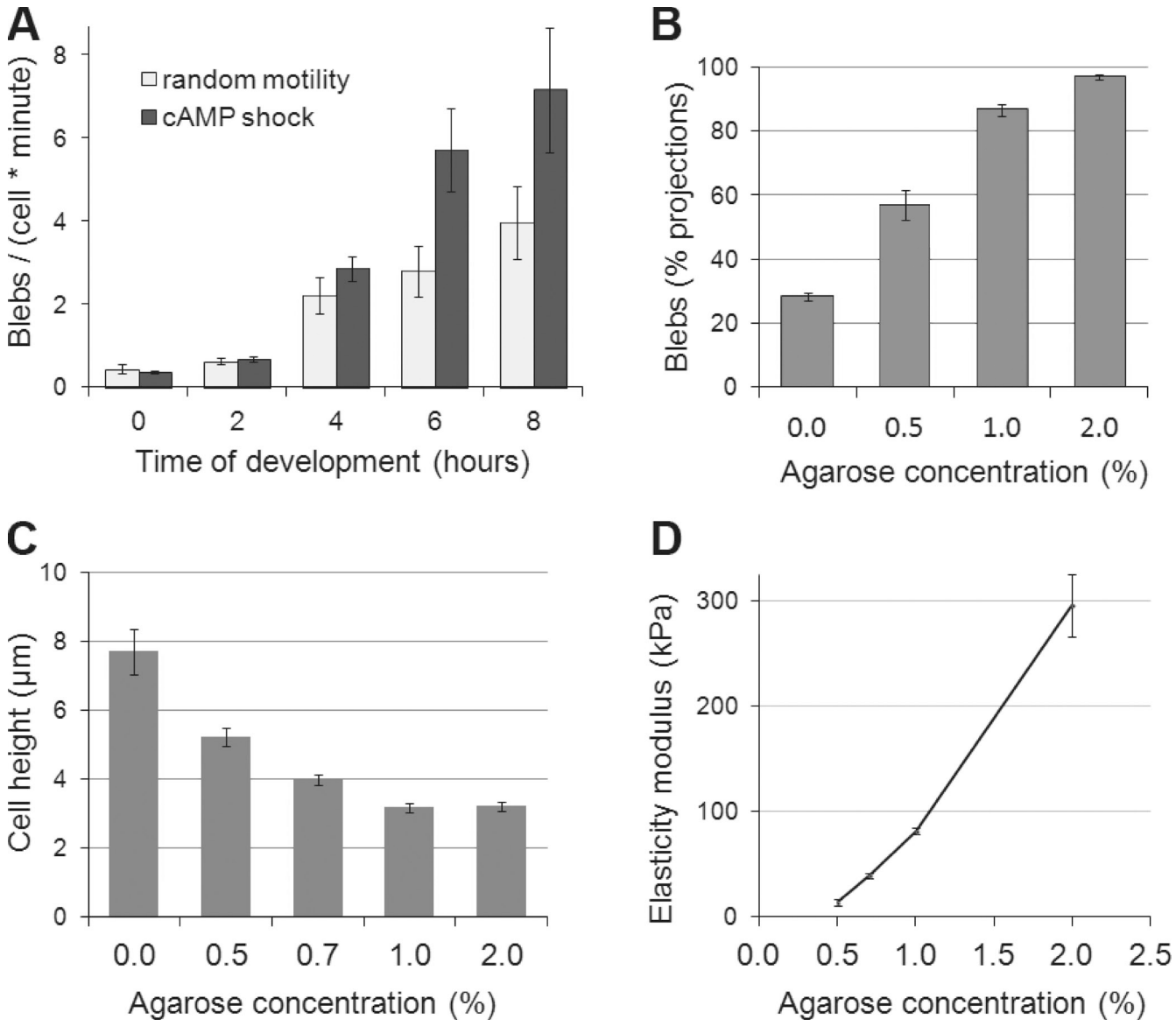

Figure 3. **Parameters regulating bleb-driven movement.** (A) Blebbing increases as cells prepare for multicellular development. Bleb frequency was measured after different times of starvation (with cyclic-AMP pulsing) in cells randomly moving under buffer, or after addition of 1 µM cyclic-AMP; results are the mean of three separate experiments, in each of which 40–80 cells were analyzed at each time-point. (B) Blebbing increases as the concentration of agarose in the overlay is increased. Blebs given as percentage of total projections (blebs + pseudopods). (C) Decreasing cell height with increasing agarose concentration in the overlay, as determined from confocal images (see Video 5 for reconstructions of cells at different agarose concentrations and for the movement of fluorescent beads in the agarose as cells pass). (D) Dependence of Young's modulus on the agarose concentration. Agarose elasticity modulus was measured by indentation with a spherical tip at 0.06 mm/s; average of three replicates for each concentration. Ax2 cells expressing the F-actin reporter ABD-GFP, to help bleb identification, were used throughout.

including fluorescent dye (RITC-dextran) in the agarose as a negative stain (Fig. 2 B; and Video 6). Both blebs and pseudopods form under these conditions, and we initially analyzed reference sets with software based on QuimP10 and using the electrostatic contour migration method to analyze the fast and small displacements of the plasma membrane during blebbing (Tyson et al., 2010).

Bleb expansion is very abrupt, lasting only about half a second, with the peak projection speed of 1.78 ± 0.74 µm/s (mean ± SD; n = 37; fastest speed of 4.93 µm/s) being approximately three times faster than actin-driven pseudopods (0.59 ± 0.23 µm/s; n = 88; fastest of 1.15 µm/s). In most cases blebs appeared as spherical caps with a height of 0.93 ± 0.11 µm, average bleb surface area of ∼8.3 µm^2, or roughly 1.8% of total cell surface area, and average bleb volume of 3.0 µm^3, or 0.5% of total cell volume (assuming S = 450 µm^2 and V = 600 µm^3; Traynor and Kay, 2007).

Blebs and pseudopods have characteristically different actin dynamics: F-actin remains continuously associated with the membrane as pseudopods expand, whereas in blebs it is sharply reduced as the bleb detaches from the cortex (Fig. 4 A). Cortical F-actin was estimated during bleb formation using QuimP10 software to measure ABD-GFP fluorescence within 0.7 µm of the membrane: the fluorescence drops by 78.0 ± 6.3% during

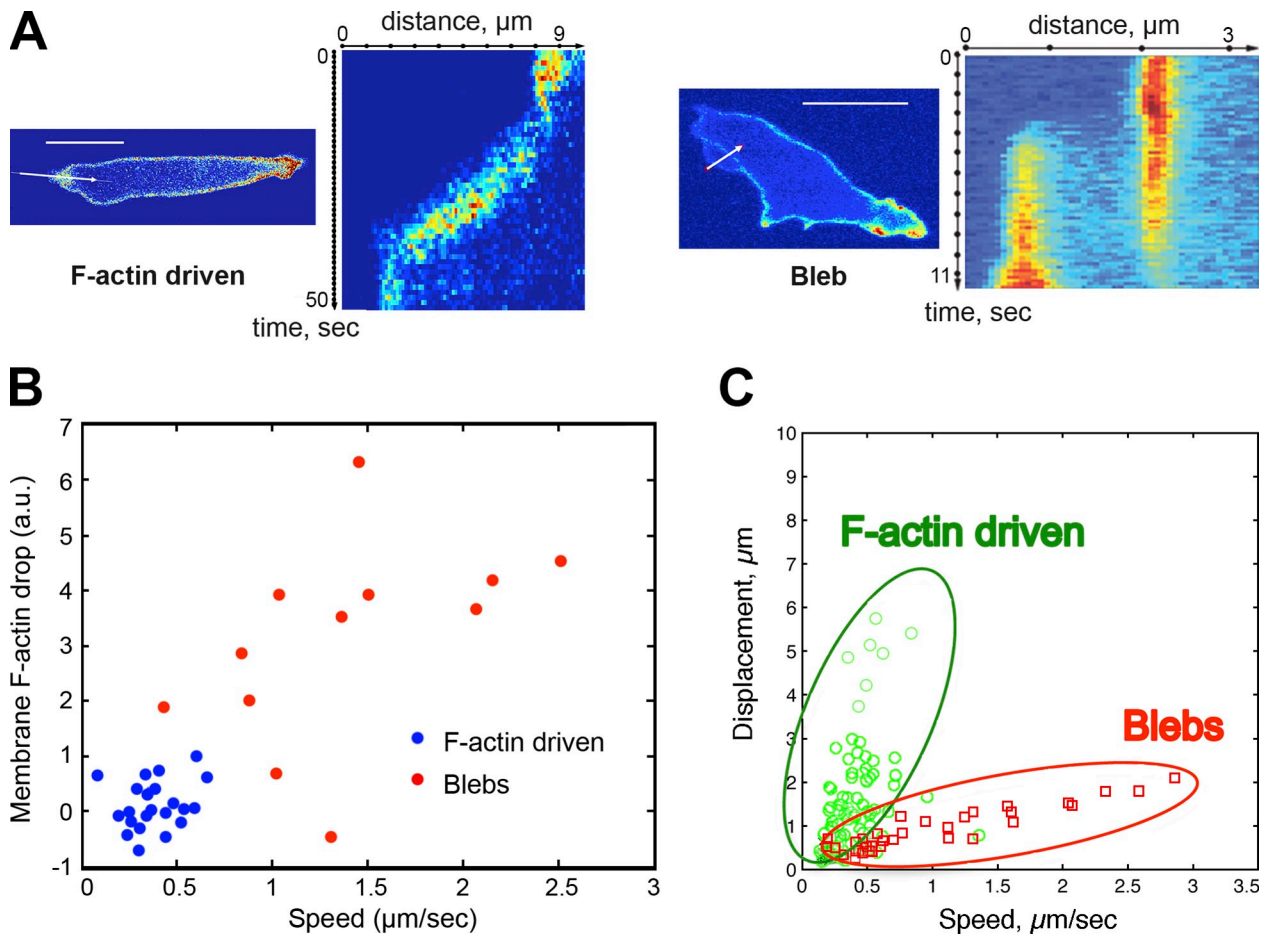

Figure 4. **Dynamics of blebs and pseudopods.** (A) Space-time plots comparing F-actin dynamics in a pseudopod and a bleb. Pseudopods are marked by a continuous, steady advance of F-actin at the leading edge, in contrast to the discontinuous advance in blebs. (B and C) Blebs are distinguished from pseudopods by their greater maximum speed of expansion, loss of F-actin at the membrane during expansion, and lower displacement achieved over their lifetime. For C, a set of 12 Ax2 cells expressing ABD-GFP and starved for 5–6 h was observed by spinning-disc confocal microscopy at 4.5 frames per second and analyzed by modified QuimP10 software (37 blebs; 88 pseudopods); loss of F-actin (B) was measured in manually identified projections from these same cells (12 blebs; 22 pseudopods). Each data-point represents a single bleb or pseudopod.

the first 2 s of bleb expansion, but by only 15.5 ± 16.7% as pseudopods expand. Combining peak speed of expansion and greatest loss of F-actin in a scatter plot allows blebs and pseudopods to be distinguished as two largely separate populations, with high-speed blebs characterized by a large drop in F-actin reporter fluorescence, whereas slow pseudopods have little, if any, decrease (Fig. 4 B). Blebs and pseudopods also differ in the total membrane displacement produced: blebs have higher speed but produce a smaller displacement, whereas pseudopods expand more slowly but cover longer distances (Fig. 4 C).

Chemotactic gradients can specify where blebs form

To test whether chemotactic gradients can specify where blebs form, we first examined cells moving under 0.7% agarose toward a source of cyclic-AMP. These cells are strongly chemotactic, and there is matching chemotactic orientation of blebbing, with most blebs forming at the front of the cell and almost none at the rear. The distribution of blebs is bimodal, with blebs most often forming either side of the true direction of the gradient, in contrast to the unimodal distribution of pseudopods in the same population of cells (Fig. 5; statistical tests are described in the legend).

This polarized blebbing occurs in cells that are already polarized by a period of steady movement in a chemotactic gradient. We therefore asked how quickly blebbing repolarizes when cells are forced to change direction by an alteration in the direction of the chemotactic gradient.

In these re-orientation experiments, cells under buffer were attracted toward a micropipette releasing cyclic-AMP, and once they had elongated and started moving toward the micropipette, it was quickly moved to the flank of the cell, inducing a turn (Swanson and Taylor, 1982; Fig. 6, A and B; and Video 7). The micropipette produces strong gradients—1.3–2.0-fold change in cyclic-AMP concentration across a 10-μm cell (Postma and van Haastert, 2009)—in which cells turn more sharply than in shallow gradients (Andrew and Insall, 2007). Around one third of cells turned while maintaining their leading edge and were not analyzed in detail, though blebs often led the way.

In the remaining cases, the cells produced a new leading edge from their flank. Blebs frequently formed in the new direction of travel within 200 s of moving the micropipette, well

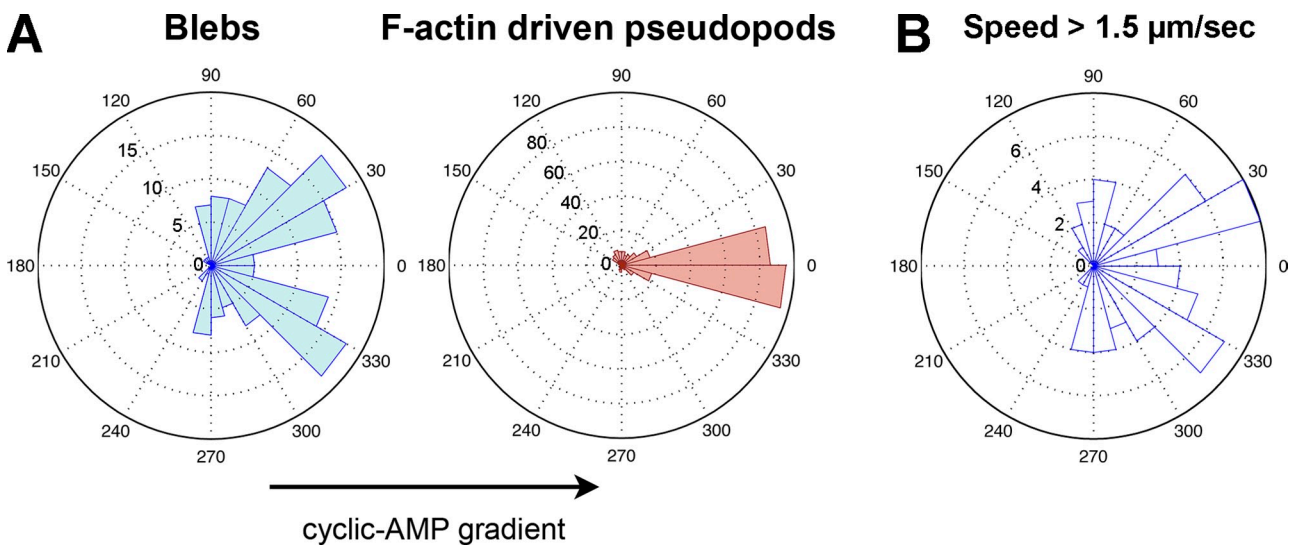

Figure 5. **Blebs are orientated by chemotactic gradients.** (A) Orientation of blebs and F-actin–driven pseudopods in cells chemotaxing toward cyclic-AMP under 0.7% agarose. Blebs and pseudopods were identified by eye (144 blebs; 304 pseudopods). (B) Orientation of all projections with a maximum speed >1.5 µm/s, equating largely to blebs, as determined using modified QuimP10 software. Both blebs and pseudopods orientate with the chemotactic gradient, but the bimodal distribution of blebs is significantly different from the distribution of pseudopods, as shown by the following statistical tests: number of blebs formed from the front and rear halves of the cell is the same, binomial distribution test: $P < 10^{-15}$; distribution of blebs and pseudopods is the same, circular Kuiper two-sample test: $P < 0.001$; unimodality of distribution, Hartigan's dip test (Hartigan and Hartigan, 1985): $P = 0.002$ for blebs and $P = 0.992$ for pseudopods; preference of pseudopods to appear at the front of the cell compared with the blebs' preference for the side, Fisher's exact test: $P < 10^{-15}$. Ax2 cells expressing the F-actin reporter ABD-GFP were used.

before the overall polarized shape of the cell was lost. Bleb formation was part of a more complex process of re-orientation, which stereotypically consisted of first, the formation of F-actin microspikes in the new direction of travel, then of blebs, and only later of F-actin–filled pseudopods (Fig. 6, C and D). This pattern varied from cell to cell (Fig. 6 E) and in some cells blebs did not form at all, but when they did, they always preceded pseudopods, and often gave rise to them by continued actin polymerization.

We conclude that the site of blebbing can be re-specified by cyclic-AMP gradients within 30 s of a change in direction of the gradient.

Genetic control of blebbing

As little is known of how blebs are triggered or chemotactically controlled, we performed a targeted genetic screen for mutants with increased or decreased blebbing. Null mutants of proteins in the cytoskeleton and cyclic-AMP signal transduction pathway were collected from the *Dictyostelium* community, and the frequency of bleb formation assessed in three different conditions: random migration under buffer to assess basal blebbing; movement under agarose to assess the effect of mechanical resistance; and global stimulation by cyclic-AMP to assess the ability of chemoattractant to induce blebbing (cyclic-AMP shock assay, in which blebbing normally follows after 20 s of adding cyclic-AMP; Video 8; Langridge and Kay, 2006). All three assays were scored qualitatively on a five-point scale and the results combined to give an overall score. Blebbing in selected mutants was also assayed more quantitatively using the QuimP10 software.

The assays used cyclic-AMP–responsive cells and each of the mutants was compared with its direct wild-type parent (Table S1, which includes further annotation of the results) and the results mapped onto current understanding of the chemotactic signal transduction network (Fig. S1; Swaney et al., 2010). We consider the results in terms of the mechanics of blebbing and the signal transduction pathways controlling it.

A prerequisite for blebbing is that the cell must produce sufficient fluid pressure to drive bleb expansion. This can be produced by myosin-II–mediated contraction of the cortex, and accordingly we find that blebbing absolutely depends on myosin-II, with heavy chain–null mutants unable to bleb under any circumstance tested, consistent with previous work (Langridge and Kay, 2006; Yoshida and Soldati, 2006). Light chain mutants are similarly unable to bleb in a cyclic-AMP shock assay or when moving under buffer or agarose (Fig. 7, A and D). Detailed analysis showed that myosin-II essential light chain–null cells (*mlcE*$^{-}$; Chen et al., 1994) completely fail to make high-speed projections, consistent with the absence of visible blebbing (Fig. 7 B). Cells of each of the myosin-II mutants also migrate more slowly than wild-type under agarose (Fig. 7 C).

Myosin-II activity in *Dictyostelium* is regulated in part through phosphorylation of its regulatory light chain, which is stimulated by cyclic-AMP signaling via downstream guanylyl-cyclases (soluble sGC and membrane-anchored GCA) and cyclic-GMP–binding proteins GbpC and GbpD (Silveira et al., 1998; Bosgraaf et al., 2005). Elimination of this cyclic-GMP–mediated signaling impairs but does not eliminate blebbing.

Several mutations impairing actin polymerization mediated through the Arp2/3 complex cause increased blebbing. These include null mutants of components of the activating SCAR–WAVE complex (Blagg et al., 2003)—Abi, Pir, HSPC300, and Scar1—but not NapA, which may have functions beyond the complex (Ibarra et al., 2006). Hypomorphic mutants of two components of the Arp2/3 complex itself (Langridge and Kay, 2007) are

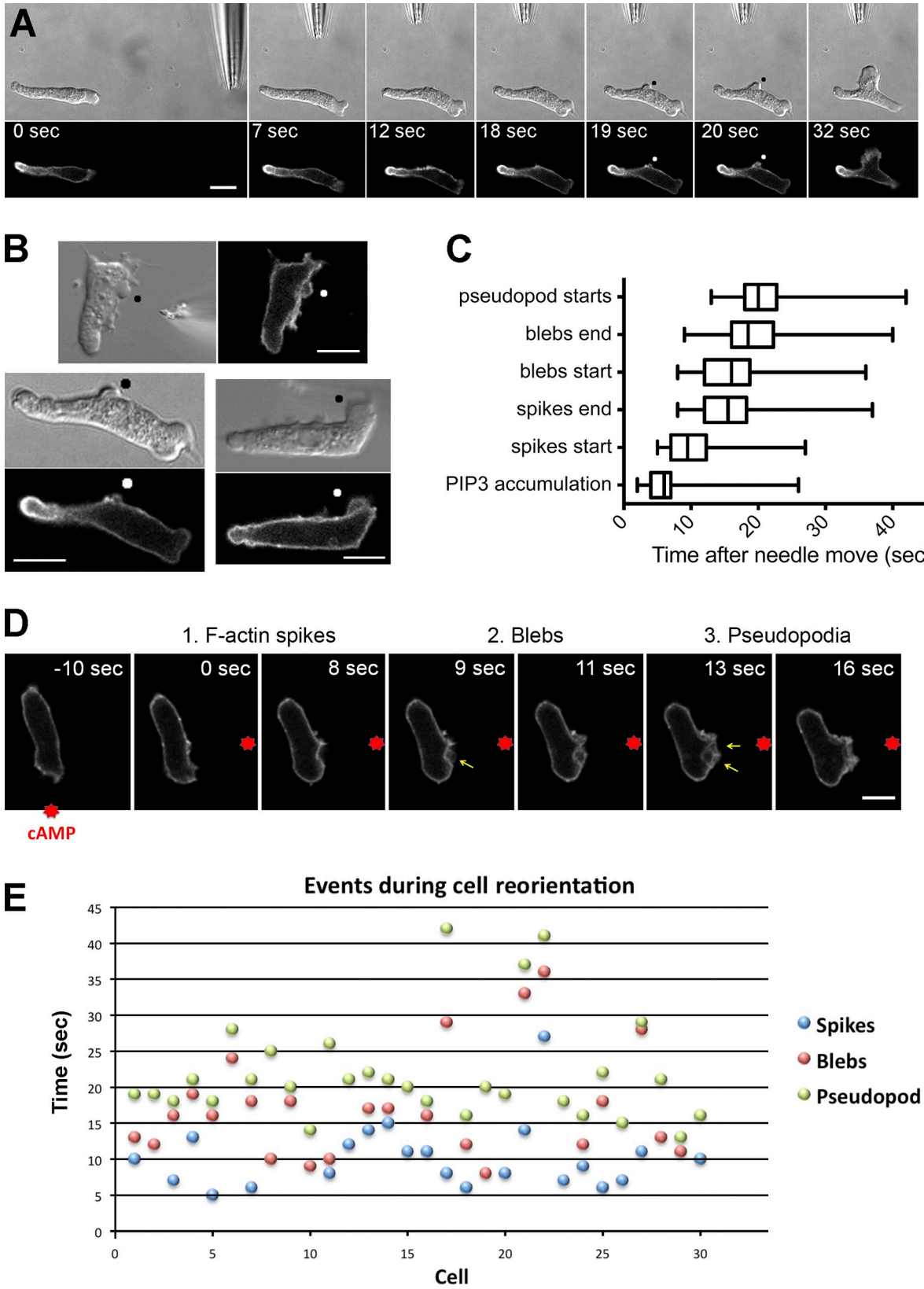

Figure 6. **Blebs rapidly re-orientate in cells chasing a micropipette releasing cyclic-AMP.** (A) Illustration of re-orientation experiment: a cell is attracted toward a needle releasing cyclic-AMP until it becomes elongated, then the needle is moved to the flank, inducing a turn. This cell follows the stereotypic pathway by first producing F-actin microspikes facing the needle (12 s), then a bleb (19 s; dot), and finally a pseudopod (32 s). (B) Examples of blebs produced during chemotactic re-orientation (see Video 7 for a selection of turning events). (C) Timing of events during re-orientation; mean and range are shown. (D) Illustration of the stereotypic sequence of events when a cell re-orientates through a new projection on its flank. Microspikes are apparent after 8 s, then at 9 s a bleb forms (single yellow arrow) and together with a second bleb, transforms into a pseudopod (double yellow arrows). (E) Behavior of 30 individual cells during re-orientation. This represents the same set of cells as in C. Only turns where the cells produce a new leading edge from their flank were analyzed. Ax2 cells were starved for ~5.5 h and express ABD-GFP, except for the cells used for PIP3 accumulation in C, which expressed CRAC-PH-GFP. Bar, 10 µm.

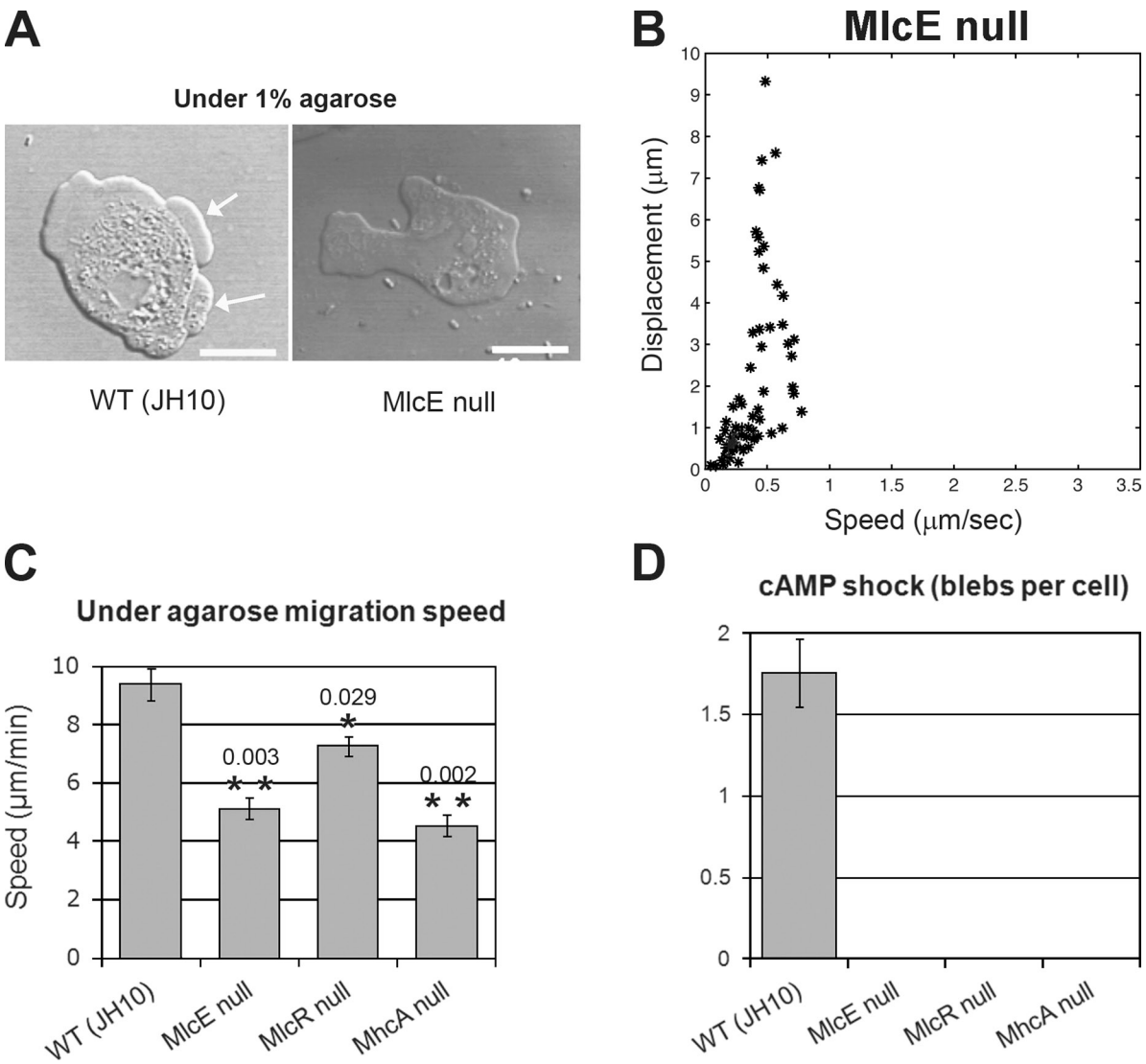

Figure 7. **Myosin-II mutants do not bleb and their movement under an agarose overlay is impaired.** (A) Cells of the parental strain, JH10, and a null mutant of myosin essential light chain (MlcE) under 1% agarose. The parental strain produces blebs (arrows), the mutant does not. (B) MlcE-null cells do not produce high-speed projections (>1.5 μm/s, equated to blebs) under a 0.7% agarose overlay (six cells analyzed using QuimP10). (C) Myosin-II null mutants move more slowly under 0.7% agarose overlays than wild-type (JH10: wild-type; MlcE: myosin essential light chain; MlcR: myosin regulatory light chain; MhcA: myosin heavy chain). (D) Myosin-null mutants do not bleb in response to uniform cyclic-AMP stimulation. Cyclic-AMP shock assay: cells under buffer were stimulated with 1 μM cyclic-AMP, and blebs counted manually (see Video 8). Under agarose migration speed: speed of cells moving under 0.7% agarose toward a well of 4 μM cyclic-AMP was measured. Bar, 10 μm.

also blebby, consistent with work on mammalian cells (Derivery et al., 2008; Bergert et al., 2012; Tozluoğlu et al., 2013). Conversely, blebbing is reduced by mutation of coronin (CorA; Shina et al., 2011) and the profilins (ProA and ProB; Haugwitz et al., 1994), whose loss may stabilize F-actin filaments or lead to F-actin over-assembly. Thus, consistent with work on mammalian cells, these results suggest a genetic antagonism between myosin-II contractility, which favors blebbing, and Arp2/3-mediated actin polymerization, which opposes it.

A second prerequisite for blebbing is that the plasma membrane must detach from the underlying cortex where a bleb forms, suggesting that mutations interfering with membrane–cortex adhesion or cortical stability will affect blebbing. Accordingly, loss of the membrane–cortex linkers talin (*talA*, *talB* double mutant; Tsujioka et al., 2008) or ponticulin (Hitt et al., 1994) increases blebbing. Talin mutant cells bleb constitutively under buffer, but are rounded and poorly adherent, so cannot penetrate under agarose and detach in the cyclic-AMP shock assay; whereas the ponticulin mutant is more adherent but only blebby in the cyclic-AMP shock assay. The significance of these differences is unknown. Many cortical proteins adhere to the plasma membrane by binding to PIP2, and loss of the predominate PI4P5-kinase, PikI, which results in cells with only 10% of wild-type levels of PIP2 (Fets et al., 2014), produces a strongly blebby phenotype under buffer, though the cells can only rarely penetrate under agarose. This mutant also has a strong defect in chemotactic signal transduction, which could contribute to the phenotype. The small G-protein, RacE, plays an essential role in cortical integrity (Gerald et al., 1998) and we find that RacE-null cells have a strong blebby phenotype, producing multiple

constitutive blebs under buffer and even more when stimulated with cyclic-AMP.

Control of blebbing by chemotactic signal transduction

We used the cyclic-AMP shock assay to investigate how chemoattractant controls blebbing (Video 8). Cyclic-AMP is perceived by a typical G-protein–coupled receptor, which through intermediate steps activates Ras GTPases and multiple downstream effectors (Swaney et al., 2010). Cyclic-AMP–induced blebbing depends on the single Gβ protein encoded in the genome (Wu et al., 1995), but surprisingly, elimination of many proteins considered central to chemotaxis has no effect (Fig. S1 and Table S1). These include components of the TORC2 complex (Lee et al., 2005), the AKT homologue PKB (Meili et al., 1999; see later), the phospholipases PLA2 (Chen et al., 2007) and PLC (Kortholt et al., 2007), and the MAP kinase ERK2 (Segall et al., 1995).

Calcium signaling is important for blebbing in zebrafish germ cells (Blaser et al., 2006), but eliminating chemotactic calcium signaling in *Dictyostelium* by knockout of the presumed IP_3 receptor, IplA (Traynor et al., 2000), has no discernable effect on blebbing.

Blebbing is regulated by PI3-kinase

In contrast, we obtained clear evidence that PI3-kinase signaling plays a crucial role in blebbing of *Dictyostelium* cells (Fig. 8). PI3-kinase signaling is abolished in a strain where all five "type-1" PI3-kinases in the genome are knocked out, and although previous work showed this strain has only minimal chemotactic defects under buffer (Hoeller and Kay, 2007), we now find that it is severely impaired in blebbing. Mutant cells make only a fraction of the number of blebs of the wild type in the cyclic-AMP shock assay, and supporting this, acute treatment of wild-type cells with the PI3-kinase inhibitor, LY-294002, also inhibits blebbing (Fig. 8 A).

PI3-kinase–null cells move more slowly under agarose than parental cells, forming pseudopods rather than blebs (Fig. 8, B and C), and produce a smaller proportion of high-speed projections, which we equate with blebs (Fig. 9 A). These projections still orientate in the chemotactic gradient, but less accurately than the wild type (Fig. 9 B).

Mutation of the PIP3 phosphatase, PTEN, which results in high PIP3 levels (Iijima and Devreotes, 2002), also impairs blebbing rather than increasing it (Table S1), suggesting that there may be an optimal level of PIP3 for efficient blebbing.

PIP3 and downstream effectors of PI3-kinase

PI3-kinases produce PIP3 in the plasma membrane within 5 s of uniform stimulation of cells with cyclic-AMP (Parent et al., 1998; Dormann et al., 2004). Similarly, a needle loaded with cyclic-AMP can induce an adjacent patch of PIP3 within 5 s of being moved to a cell, and often this is the site at which a bleb subsequently forms (Fig. 6 C, Fig. 10 A, and Video 9).

PIP3 is a docking site for downstream effector proteins, of which three, each carrying a PH domain, are particularly relevant to chemotaxis: the protein kinase PKB/AKT (Meili et al., 1999) and two less well-characterized proteins, CRAC (Insall et al., 1994; Parent et al., 1998) and PhdA (Funamoto et al., 2001). We examined mutants in each of these proteins (Fig. 8 and Table S1).

Neither a single mutant of PKB, nor a double mutant of PKB and its membrane-anchored homologue, PKBR1 (Kamimura et al., 2008), were affected in cyclic-AMP–induced blebbing (Fig. 8 A). Moreover, the PKB/PKBR1–null cells produce blebs up-gradient in re-orientation experiments (Fig. 8 D). Hence, the PI3-kinase–dependent control of blebbing is not mediated by PKB and PKBR1.

In contrast, both CRAC and PhdA mutants are impaired in blebbing. To confirm this, we quantitatively analyzed blebbing in CRAC- and PhdA-null mutants re-created in our parental strain and found that these new mutants are likewise impaired, but can be substantially rescued by overexpressing the corresponding GFP fusion protein (Fig. 8 A). PhdA and CRAC are likely to have distinct roles in PIP3 signaling because blebbing by PhdA$^-$ cells is only impaired in the cyclic-AMP shock assay, whereas it is impaired in all three assays in CRAC$^-$ cells. CRAC (but not PhdA) activates adenylyl cyclase (Insall et al., 1994) and it is notable that a null mutant of adenylyl-cyclase (Pitt et al., 1992) has a similar phenotype to CRAC (Table S1; ACA), suggesting that the CRAC phenotype may result from a lack of cyclic-AMP. Cells of a double CRAC/PhdA-null mutant are very immotile, un-polarized, and flattened compared with the wild type, and have an even stronger blebbing defect than the single mutants, producing fewer than 20% of the wild-type number of blebs in the cyclic-AMP shock assay (Fig. 8 A). This double mutant is able to re-orientate to a cyclic-AMP needle, producing a PIP3 patch and F-actin microspikes like the wild type, but rarely does this lead to a bleb (Fig. 10 B and Video 10).

CRAC and PhdA single mutants move more slowly than their parent under agarose and the double CRAC/PhdA mutant is strikingly defective, moving at only one third of the speed of the parent, without visible blebs (Fig. 8 B). Consistent with this, the CRAC/PhdA double mutant produces fewer high-speed projections than its parent, and the projections it does form are less well orientated in the chemotactic gradient, contributing further to its poor motility (Fig. 9, A and B).

Separate regulation of blebbing and actin polymerization

Because there is clear evidence that blebbing in response to cyclic-AMP is controlled through PI3-kinase, we asked whether this same pathway controls actin polymerization. Cyclic-AMP stimulation causes a burst of actin polymerization peaking after 5–10 s (McRobbie and Newell, 1983). In contrast to blebbing, this actin response is not impaired in the PI3-kinase quintuple mutant (Hoeller and Kay, 2007), or in the PhdA/CRAC double mutant after either global or local stimulation (Fig. 9, C and D; and Fig. 10 B). We conclude that the acute blebbing and actin responses to cyclic-AMP are mediated through significantly different signal transduction pathways.

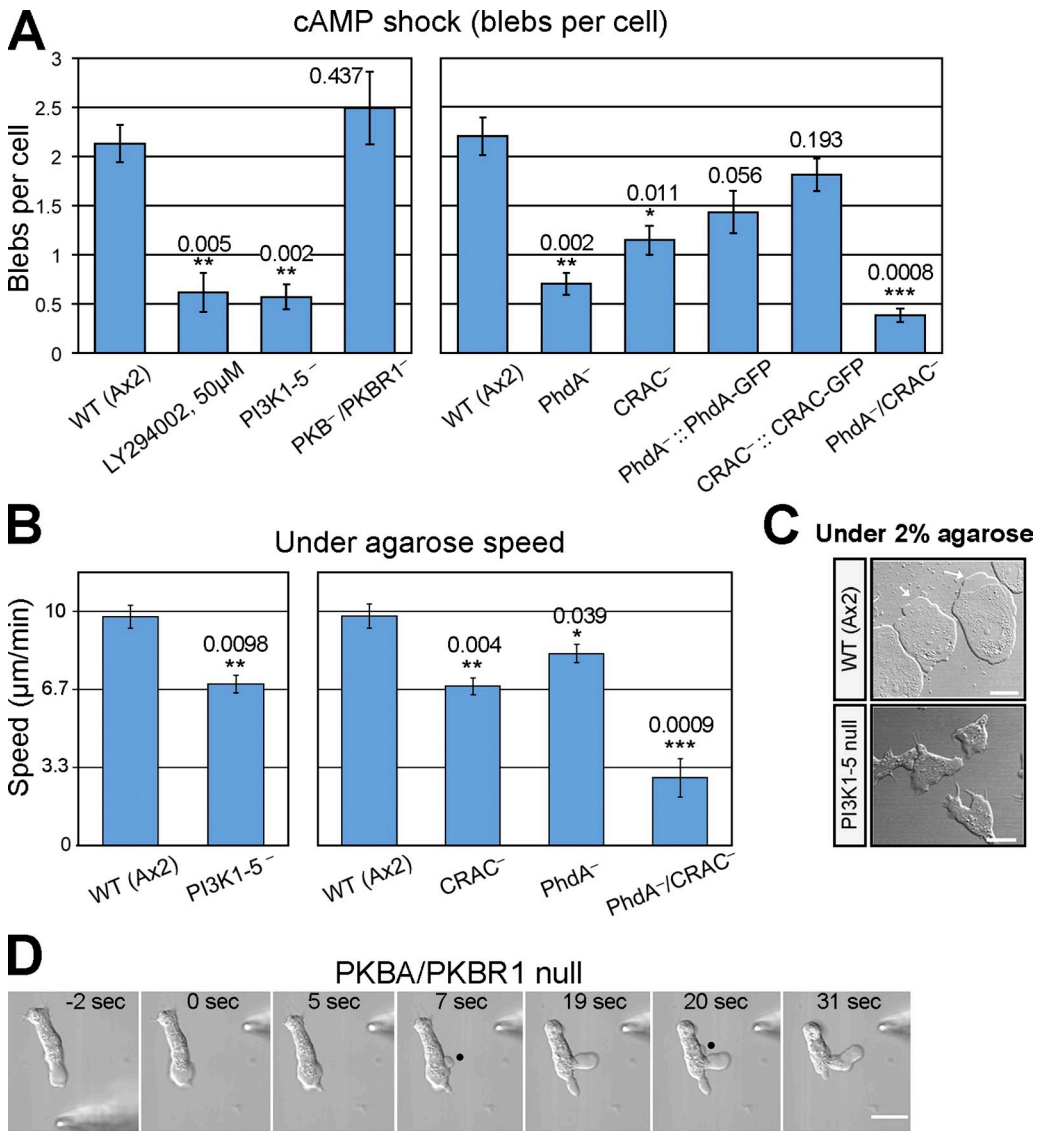

Figure 8. **Blebbing and movement under an agarose overlay are regulated by PI3-kinase and its downstream effectors, CRAC and PhdA.** (A) Blebbing in response to cyclic-AMP is severely impaired when PI3-kinase activity is inhibited, either in a mutant lacking five PI3-kinases (PI3K1–5⁻) or by adding the PI3-kinase inhibitor, LY294002, to Ax2 cells. Blebbing in mutants of downstream PIP3-binding proteins is unimpaired in PKB/PKBR1 double-null cells, but significantly impaired in CRAC⁻ and PhdA⁻ cells, where it can be substantially rescued by re-expression of the corresponding GFP fusion protein. A double CRAC/PhdA-null mutant blebs very poorly. (B) Movement speed is reduced under 0.7% agarose overlays in PI3-kinase, CRAC, and PhdA mutants. (C) Wild-type and PI3-kinase quintuple knock-out cells under 2% agarose. (D) PKB/PKBR1 double-mutant cell produces a bleb (dot) in a re-orientation experiment performed as in Fig. 6, and providing evidence that blebbing is unimpaired in this mutant. Cyclic-AMP shock assay: cells were stimulated with 1 μM cyclic-AMP, and blebs counted manually. Under agarose migration speed: the speed of cells moving under 0.7% agarose toward a well containing 4 μM cyclic-AMP was measured. Bar, 10 μm.

Discussion

The leading edge of *Dictyostelium* cells can be advanced by the formation of small, rapidly expanding blebs, as well as by F-actin–driven pseudopods and microspikes. The blebs are usually smaller and shorter-lived than their mammalian counterparts (Charras et al., 2008), with a life cycle of less than 10 s, from projection through to consolidation by an F-actin cortex (Langridge and Kay, 2006; Yoshida and Soldati, 2006; this paper). Blebs are clearly distinguishable from pseudopods by their smooth, rounded shape, greater speed of projection, lack of F-actin during expansion, and F-actin scar, but frequently coexist with pseudopods at the leading edge forming hybrid structures, and can even give rise to pseudopods by continued actin polymerization.

By inducing cells to move under an agarose overlay (Laevsky and Knecht, 2001), we have found a simple and informative way of switching them to bleb-driven migration. From the arguments advanced in the results, we propose that mechanical resistance alone is sufficient to cause *Dictyostelium* cells to move using blebs.

The switch from pseudopods to blebs occurs within minutes, as cells move under the overlay. In principle it might be explained if blebs could produce more force than pseudopods, allowing them to expand better than pseudopods against mechanical resistance. Equally, cells may sense mechanical resistance

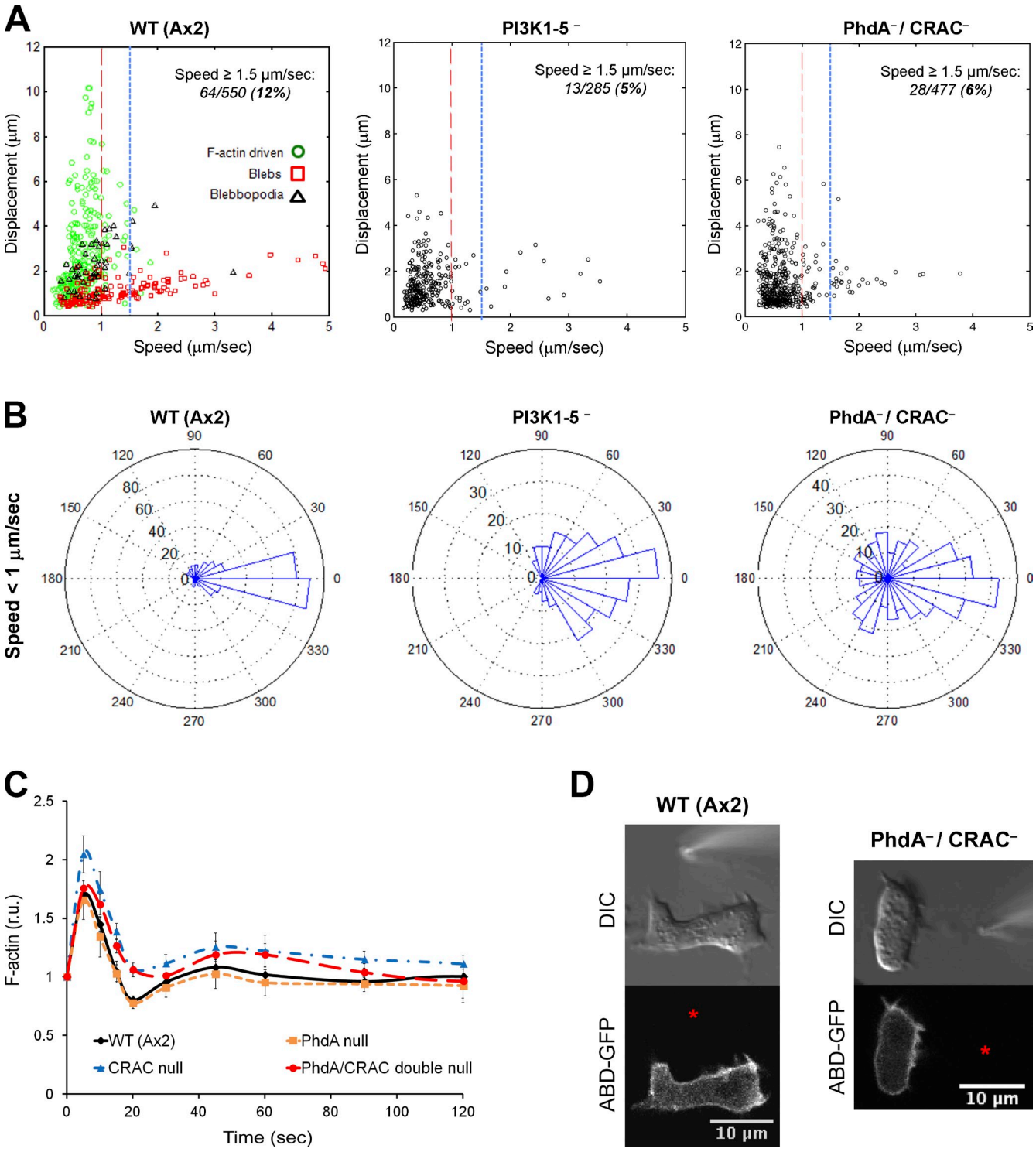

Figure 9. **Protrusions made by cells impaired in PI3-kinase signaling.** (A) Blebbing is impaired in mutant cells chemotaxing under 0.7% agarose. Analysis with QuimP10 shows that the mutants are deficient in forming high-speed projections, which we equate to blebs (cells analyzed: Ax2 = 30; PI3K1–5^{-} = 19; CRAC^{-}/PhdA^{-} = 19). Projections made by the wild type were further classified by eye as pseudopods or blebs (green and red) or various hybrids and unidentified (other marks). (B) Chemotactic orientation of low-speed projections (<1 µm/s, equated to pseudopods) of cells moving under 0.7% agarose. It is apparent that pseudopods are projected less accurately by the mutants (projections analyzed: Ax2 = 374; PI3K1–5^{-} = 257; CRAC^{-}/PhdA^{-} = 416). (C) Actin polymerization after acute stimulation of cells with cyclic-AMP. The PhdA and CRAC mutants show a robust fast response (peak before 10 s), similar to the wild type. (D) Formation of F-actin microspikes during turning toward a micropipette releasing cyclic-AMP (red asterisks). Microspikes form in the same time-scale as the first peak of actin polymerization in C and are made by the PhdA/CRAC double mutant as well as the wild type. In A and B, projections by cells moving under 0.7% agarose were identified automatically using modified QuimP10 software and their maximum speed, total displacement, and orientation determined.

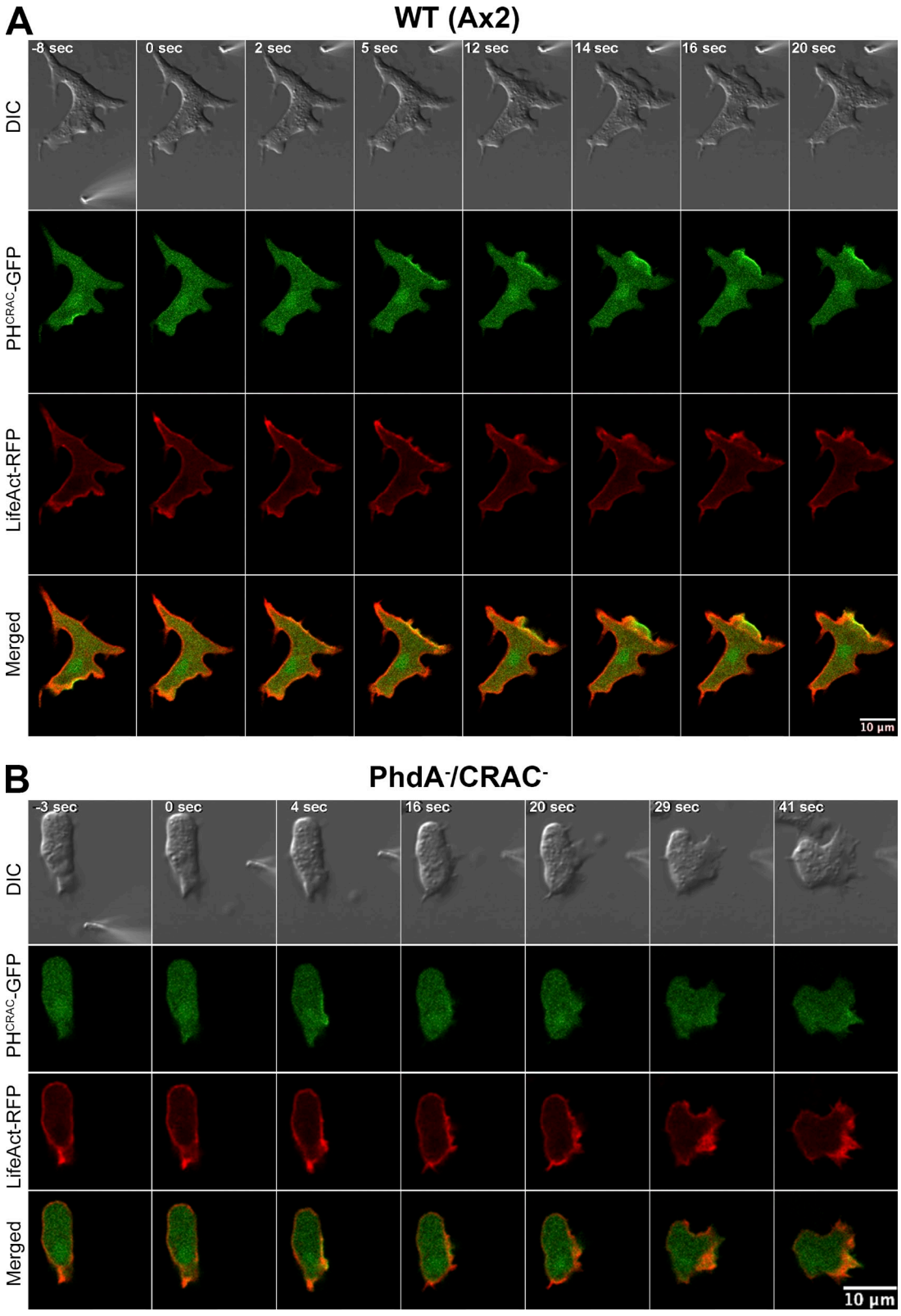

Figure 10. **PIP3, F-actin structures, and blebs during re-orientation of wild-type and PhdA/CRAC double-null cells.** (A) Re-orientation of a wild-type cell. PIP3 accumulates at the membrane adjacent to the cyclic-AMP micropipette within 5 s of the micropipette movement, and F-actin microspikes form at the same time. At 14 s after the move a substantial bleb forms from the region of the membrane with highest PIP3 accumulation (see Video 9). (B) Re-orientation of a PhdA^{-}/CRAC^{-} double-mutant cell. These cells are generally less elongated than the wild type, but can still turn by forming a new leading edge from their flank. Although a PIP3 patch and F-actin microspikes form normally, the cell does not turn with a bleb, but uses a pseudopod instead (see Video 10). Turning experiments, using a micropipette filled with cyclic-AMP, were performed as in Fig. 6 with wild-type and HM1589 cells expressing PH-CRAC-GFP and LifeAct-RFP, and starved for 5.5 h.

and then use a signaling mechanism to alter the balance between actin polymerization and myosin contractility, thus increasing cellular pressure and favoring bleb formation (Sanz-Moreno et al., 2008). The idea that the balance between actin polymerization and myosin contractility regulates blebbing is supported by previous work from mammalian cells (Derivery et al., 2008; Bergert et al., 2012; Tozluoğlu et al., 2013) and by our finding of increased blebbing in SCAR–WAVE and Arp2/3 complex mutants.

We have shown that chemotactic gradients can control bleb positioning, consistent with earlier observations in fish embryos (Fink and Trinkaus, 1988; Blaser et al., 2006). In under-agarose experiments, blebs are strongly polarized up-gradient, with an intriguingly bimodal distribution either side of the gradient direction. In contrast, pseudopods are unimodally up-gradient, and blebs formed under 2% agarose—where fewer pseudopods form—are less clearly bimodal (unpublished data). This suggests that the two types of projection may interact, perhaps with blebs preferentially forming on the flanks of pseudopods (see later).

Cells can track a micropipette releasing cyclic-AMP, and turn when it moves (Swanson and Taylor, 1982). Turning cells often produce a new leading edge from their flank, stereotypically by first making F-actin microspikes, then blebs within 20 s, and finally pseudopods. This sequence suggests a causative relationship in which microspikes trigger blebs, and then blebs trigger pseudopods by continued actin polymerization. Whatever the exact causal relationship between these events, the experiment demonstrates that bleb positioning is under direct chemotactic control. Our work sheds light on two aspects of how this might be achieved.

PIP3 is produced in the plasma membrane a few seconds after cells are stimulated with cyclic-AMP (Parent et al., 1998; Dormann et al., 2004), and ∼20 s before blebs form. We find that blebbing is severely inhibited when PIP3 production is impaired, either in a quintuple PI3-kinase mutant with only ∼10% of wild-type levels of PIP3 (Hoeller and Kay, 2007; Hoeller et al., 2013) or by a PI3-kinase inhibitor. Downstream of PIP3, efficient blebbing depends on two PH domain proteins, CRAC and PhdA (Insall et al., 1994; Parent et al., 1998; Funamoto et al., 2001), but not on the protein kinase, PKB (Meili et al., 1999). Consistent with their blebbing defects, the PI3-kinase quintuple and CRAC/PhdA double mutants move slowly under agarose compared with wild-type, producing projections less accurately and with fewer at high speed, and though the double mutant turns toward a cyclic-AMP micropipette, making microspikes and pseudopods, it rarely blebs.

We are less certain whether PI3-kinases convey spatial information to specify where blebs form, or have a more general effect, such as controlling myosin contractility. In the case of cells stimulated with a cyclic-AMP micropipette, blebs often form at PIP3 patches, but we do not see such a correlation in cells chemotaxing under agarose (unpublished data), where some blebs are triggered independently of detectable PIP3 patches.

In contrast to blebbing, actin polymerization is stimulated by cyclic-AMP independently of PI3-kinase (Hoeller and Kay, 2007) or CRAC and PhdA (this paper). Thus, blebbing appears to be regulated through a signaling module consisting of PI3-kinase, CRAC, and PhdA, distinct from the pathway controlling actin polymerization. At odds with this idea, a mutant lacking three related PIP3-binding myosin-I proteins is impaired in actin polymerization as well as blebbing (Table S1; Chen et al., 2012). Possibly, the myosin-I proteins either regulate actin polymerization independently of PIP3, or are PIP3 dependent, but serve a permissive function for which residual PIP3 in the PI3-kinase mutant is sufficient (Hoeller et al., 2013).

Blebs form by detachment of the plasma membrane from the underlying cortex (Charras et al., 2008). This might be triggered by physical rupture of the cortex (Tinevez et al., 2009), or by reduction of membrane–cortex adhesion, due to PIP2 breakdown (Raucher et al., 2000). We see no evidence for cortical rupture in *Dictyostelium* blebs—the cortex appears to remain intact as a scar for a few seconds after blebs form—but our genetic evidence shows that PIP2 levels are relevant to bleb formation because the greatly reduced PIP2 levels in the PI4P5-kinase mutant (Fets et al., 2014) cause increased blebbing. However, global stimulation of cells with cyclic-AMP does not cause a detectable drop in PIP2 levels, suggesting that changes in PIP2 are not the physiological trigger of blebbing in this case. In contrast, PI3-kinase activity is sharply localized in migrating cells, suggesting that local depletion of their substrate, PIP2, could trigger blebbing.

Our observations also suggest an alternative, purely physical route for triggering blebs, based on the relief of local membrane stress. We noticed that cells moving under agarose usually bleb at areas of negative membrane curvature, often on the flanks of earlier projections; while in re-orientation experiments, the first step in a cell changing direction is the formation of F-actin microspikes, which also produce strong local membrane curvature, and are often followed by blebs a few seconds later. We suggest in both cases that negative curvature produces membrane stress, which can be relieved by making a bleb. This mechanical coupling of blebs and membrane curvature may allow actin dynamics to indirectly control where blebs form (unpublished data).

The increase in blebbing in early development is underpinned by increased expression of myosin-II, CRAC, and PhdA (Parikh et al., 2010) and may equip cells for later development, when they have to move within a tightly packed, multicellular mass. This is particularly important for pre-stalk cells, which sort out from scattered positions within the mass to make a coherent tissue (Kay and Thompson, 2009) and express myosin-II to especially high levels (Maeda et al., 2000). Bleb-driven movement has not been reported within multicellular aggregates (Dormann et al., 2004) but cells released from them move largely with blebs (Yoshida and Inouye, 2001), and it is notable that several mutants that are defective in blebbing (this paper) are also defective in morphogenesis (Hitt et al., 1994; Knecht and Loomis, 1988; Tsujioka et al., 1999; Wang et al., 1999).

The ability of *Dictyostelium* cells to move with either blebs or pseudopods complicates the analysis of chemotactic mechanisms, and may account for some of the redundancy evident from genetic analysis. But equally, the ability to evoke and study bleb-driven motility in such an amenable system opens new routes to answering fundamental questions about this type of movement.

Materials and methods

Strains, cultivation conditions, and reporters

In most experiments the axenic strain Ax2 (Kay laboratory strain; DBS0235521 at http://dictybase.org) of *Dictyostelium discoideum* was used as wild type and all experiments were at 22°C. Cells were grown in HL5 axenic medium (ForMedium) or on SM plates in association with bacteria (Kay, 1987).

Mutant strains were obtained from the Dicty Stock Center (http://dictybase.org/StockCenter/StockCenter.html), or by individual donation, as detailed in Table S1. Knockout strains of PhdA (*phdA*$^-$; HM1650) and CRAC (*dagA*$^-$, HM1649) and the double mutant (*phdA*$^-$, *dagA*$^-$; HM1659) were created in strain Ax2 (Kay laboratory) by homologous recombination and recycling of the selective marker (Faix et al., 2004).

The ABD-GFP F-actin reporter construct consists of the F-actin–binding domain of ABP-120 (residues 9–248) fused to GFP and driven by the actin15 promoter (Pang et al., 1998); transformation into Ax2 gave strain HM2231. ABD-GFP expression was maintained by growth in medium containing 10 µg/ml of G418 antibiotic. The cAR1-GFP reporter, used as a plasma membrane marker, utilizes the full-length cyclic-AMP receptor-1 coding sequence fused to GFP in the pJK1 extrachromosomal expression vector (Xiao et al., 1997). A double reporter for PIP3 and F-actin was constructed by D. Veltman: the act6 promoter driving the hygromycin resistance marker of pDM448 (Veltman et al., 2009) was replaced by the *coaA* promoter, which is more active during growth on bacteria, yielding pDM1045. The PIP3-binding domain of CRAC (residues 1–126 of the *dagA* gene) was then ligated into the cloning site as a BamHI–XbaI fragment, yielding pDM1113. An expression cassette with Lifeact-mRFPmars was created by ligating a linker encoding Lifeact into the BglII–SpeI site of pDM330 (Veltman et al., 2009), yielding pDM623. This cassette was excised with NgoMIV and ligated into pDM1113 to generate the dual expression vector pDM1133.

Live-cell microscopy and image analysis

All microscopy experiments were performed under KK2 buffer (16.5 mM KH_2PO_4, 3.8 mM K_2HPO_4, 2 mM $MgSO_4$, and 0.1 mM $CaCl_2$). Aggregation-competent cells were prepared by shaking freshly harvested cells at 2×10^7 cells/ml in KK2 at 180 rpm at 22°C for 1 h and then pulsing with 70–90 nM cyclic-AMP (final concentration after a pulse) every 6 min for a further 4.5 h (RasC$^-$/RasG$^-$ double-null strain and CRAC-null cells were pulsed with 400 nM cyclic-AMP as they are defective in cyclic-AMP relay). After this time, small clumps of cells form and stick to the flasks giving a morphological check for adequate development.

Cells were imaged on Lab-Tek coverslips (Thermo Fisher Scientific) using an inverted laser-scanning confocal microscope (model 710 or 780; Carl Zeiss) with a 63×/1.4 NA oil immersion objective, with images collected using Zen software (Carl Zeiss) and processed using ImageJ (National Institutes of Health), or a spinning-disk confocal microscope (Ultraview; PerkinElmer) on an inverted microscope body (model IX71; Olympus) with a 100×/1.4 NA oil immersion objective and a CCD camera (Orca ER; Hamamatsu Photonics).

Cell outline segmentation and membrane protrusion analysis were performed using modified QuimP10 software (http://www.warwick.ac.uk/QuimP) based on the electrostatic contour migration method (Tyson et al., 2010).

Blebbing assay

Blebbing was assayed after addition of 1 µM cyclic-AMP to aggregation-competent cells (Langridge and Kay, 2006) imaging every 1 s for 2 min. Blebbing occurred between 20 and 50 s after cyclic-AMP addition and blebs were summed over this period.

Under-agarose assay

A modified version of the under-agarose assay method was used (Laevsky and Knecht, 2001). A thin layer (750 µl) of 0.5–2.0% SeaKem GTG agarose (Lonza) in KK2 was poured into preheated, two-chamber Lab-Tek coverslips (surface area of each chamber = 4.2 cm^2), and once it had set, three parallel, rectangular troughs were cut 6 mm apart. The central trough was 4 mm wide and 8 mm long; the side ones 1 × 5 mm. To the central trough, 4 µM cyclic-AMP was added and left for 40 min to allow a gradient to be set up within the agarose layer, after which 10^5 aggregation-competent cells were placed in each side trough. For negative staining, rhodamine-B isothiocyanate–dextran was added to the agarose at 0.5 mg/ml. To estimate the speed of cell migration under agarose, images were collected every 5 s for 1 h using a microscope (Axiovert S100; Carl Zeiss) with a 10× objective and a motorized stage. Migration speed was calculated as the average displacement (distance from start-point to end-point) of 20 leading cells toward the source of chemoattractant during 1 h.

Agarose elasticity modulus was measured with an Instron 5544 microindenter system (Instron), by indentation with a 4.5-mm spherical tip at 0.06 mm/s. Compression type testing was done using a feedback-based load control with a ramp-hold load profile, incorporating a rise time of 15 s and hold time of 1 min. The values were obtained as load versus extension and used to calculate the stiffness of the gel by considering the contact of the indenting sphere with the agarose gel as a nonadhesive elastic contact. A Hertz model was then used to describe the contact between sphere and an elastic half-space. The data are plotted as average of three replicates for each agarose concentration ± SEM.

Re-orientation assay

Cells transformed with ABD-GFP were settled in Lab-Tek microscopy chambers (Thermo Fisher Scientific) in KK2 buffer, and a micropipette (Femtotips II; Eppendorf) loaded with 2 µM cyclic-AMP was placed ∼40 µm from a cell. Once the cell became polarized and started moving toward the micropipette, the micropipette was rapidly moved (in 1–2 s) to the middle of the cell's flank at a distance of ∼10–15 µm from the cell surface. The process of reorientation was filmed at 1 frame per second; $n = 30$ cells were analyzed.

Mutant screening

Aggregation-competent cells of mutant strains (Table S1) were compared with their direct parents in three different assays. "Under buffer": the frequency of blebs compared with actin-driven pseudopodia in randomly moving cells moving on a coverslip under KK2 buffer; "under-agarose": the frequency of blebs compared with actin-driven pseudopodia in cells chemotaxing to cyclic-AMP under 0.7% agarose and, in selected cases, the speed of under-agarose chemotaxis determined from time-lapse movies; and "cyclic-AMP shock": the frequency of blebbing induced by cyclic-AMP shock. Results from the assays were combined using the following scoring system: "0": mutant not distinguishable from its parent; "−": mutant blebs (or moves under agar) slightly less well than its parent; "− −": mutant does not bleb at all, or very weakly (moves much more slowly under agarose). Similarly, strains that bleb slightly more, and much more than their parent received scores of "+" and "+ +", respectively. The blebbing scores are finally summed for all three assays to give a composite score for each strain. The assays were performed in triplicate and for each repeat, 30–50 cells from several different microscopy chambers were analyzed for each set of experimental conditions.

F-actin polymerization assay

Actin polymerization in response to cyclic-AMP was measured in suspensions of aggregation-competent cells by a modification of previous methods (Hall et al., 1988). At each time-point, 3×10^6 cells in 200 µl KK2 were stimulated with 1 µM cyclic-AMP and the fix/stain buffer (25 mM Pipes, 5 mM EGTA, 2 mM $MgCl_2$, pH 6.8, 3% formaldehyde, 0.24% Triton X-100, and 0.6 µM TRITC-phalloidin) added at the appropriate time. The sample was mixed at room temperature for 20 min and the Triton-insoluble cytoskeleton was pelleted in a microfuge at maximum speed for 2 min. The supernatant was aspirated off and the pellet washed in 25 mM Pipes, 5 mM EGTA, 2 mM $MgCl_2$, pH 6.8, and 0.1% saponin for 30 min at room temperature. The cytoskeleton was pelleted as before and the TRITC-phalloidin extracted in 1 ml methanol by vigorous shaking for 15 min, and the fluorescence was measured.

Statistical analysis

Results of the blebbing and under-agarose assays for different strains were compared using unpaired two-tailed Student's *t* tests. Differences were considered significant at $P < 0.05$. Other statistical tests are described in the text.

Online supplemental material

Fig. S1 shows the results of the blebbing mutant screen mapped onto a scheme for cyclic-AMP signal transduction. Video 1 shows a typical cell using both blebs and pseudopods to move under buffer. Video 2 shows a bleb transforming into a pseudopod. Video 3 shows a stream of cells in which the leader moves purely with blebs. Video 4 depicts a cell moving under agarose showing pure bleb-driven movement. Video 5 shows 3D reconstructions of cells moving under different agarose concentrations, and the deflection by passing cells of beads embedded in the agarose. Video 6 shows a cell moving under agarose containing fluorescent dye to reveal its outlines. Video 7 shows examples of cells turning to a cyclic-AMP needle. Video 8 shows blebbing caused by adding cyclic-AMP. Video 9 shows a cell expressing reporters for PIP3 and F-actin turning toward a needle

releasing cyclic-AMP. Video 10 shows CRAC/PhdA double-mutant cells, expressing reporters for PIP3 and F-actin, turning toward a needle releasing cyclic-AMP. Table S1 gives the result of the screen for blebbing mutants, including comments on the assays used and on the results for individual mutants. Online supplemental material is available at http://www.jcb.org/cgi/content/full/jcb.201306147/DC1. Additional data are available in the JCB DataViewer at http://dx.doi.org/10.1083/jcb.201306147.dv.

We are very grateful to members of the *Dictyostelium* community and the *Dictyostelium* Stock Center for strains listed in Table S1; A. Kabla and N. Srivastava (Cambridge University Engineering Department) for elasticity measurements; members of the LMB Dicty group for valuable discussions; and especially D. Traynor for strain creation and N. Barry for help with microscopy.

We acknowledge the MRC for core support (MRC file reference number U105115237), a Herchel Smith Fellowship to E. Zatulovskiy, and Warwick Systems Biology DTC support for R. Tyson.

The authors declare no competing financial interests.

Submitted: 25 June 2013
Accepted: 30 January 2014

References

Andrew, N., and R.H. Insall. 2007. Chemotaxis in shallow gradients is mediated independently of PtdIns 3-kinase by biased choices between random protrusions. *Nat. Cell Biol.* 9:193–200. http://dx.doi.org/10.1038/ncb1536

Arrieumerlou, C., and T. Meyer. 2005. A local coupling model and compass parameter for eukaryotic chemotaxis. *Dev. Cell.* 8:215–227. http://dx.doi.org/10.1016/j.devcel.2004.12.007

Bergert, M., S.D. Chandradoss, R.A. Desai, and E. Paluch. 2012. Cell mechanics control rapid transitions between blebs and lamellipodia during migration. *Proc. Natl. Acad. Sci. USA.* 109:14434–14439. http://dx.doi.org/10.1073/pnas.1207968109

Blagg, S.L., M. Stewart, C. Sambles, and R.H. Insall. 2003. PIR121 regulates pseudopod dynamics and SCAR activity in *Dictyostelium. Curr. Biol.* 13:1480–1487. http://dx.doi.org/10.1016/S0960-9822(03)00580-3

Blaser, H., M. Reichman-Fried, I. Castanon, K. Dumstrei, F.L. Marlow, K. Kawakami, L. Solnica-Krezel, C.P. Heisenberg, and E. Raz. 2006. Migration of zebrafish primordial germ cells: a role for myosin contraction and cytoplasmic flow. *Dev. Cell.* 11:613–627. http://dx.doi.org/10.1016/j.devcel.2006.09.023

Bloomfield, G., Y. Tanaka, J. Skelton, A. Ivens, and R.R. Kay. 2008. Widespread duplications in the genomes of laboratory stocks of *Dictyostelium discoideum. Genome Biol.* 9:R75. http://dx.doi.org/10.1186/gb-2008-9-4-r75

Bosgraaf, L., A. Waijer, R. Engel, A.J. Visser, D. Wessels, D. Soll, and P.J. van Haastert. 2005. RasGEF-containing proteins GbpC and GbpD have differential effects on cell polarity and chemotaxis in *Dictyostelium. J. Cell Sci.* 118:1899–1910. http://dx.doi.org/10.1242/jcs.02317

Charras, G., and E. Paluch. 2008. Blebs lead the way: how to migrate without lamellipodia. *Nat. Rev. Mol. Cell Biol.* 9:730–736. http://dx.doi.org/10.1038/nrm2453

Charras, G.T., M. Coughlin, T.J. Mitchison, and L. Mahadevan. 2008. Life and times of a cellular bleb. *Biophys. J.* 94:1836–1853. http://dx.doi.org/10.1529/biophysj.107.113605

Chen, C.L., Y. Wang, H. Sesaki, and M. Iijima. 2012. Myosin I links PIP3 signaling to remodeling of the actin cytoskeleton in chemotaxis. *Sci. Signal.* 5:ra10. http://dx.doi.org/10.1126/scisignal.2002446

Chen, L., M. Iijima, M. Tang, M.A. Landree, Y.E. Huang, Y. Xiong, P.A. Iglesias, and P.N. Devreotes. 2007. PLA2 and PI3K/PTEN pathways act in parallel to mediate chemotaxis. *Dev. Cell.* 12:603–614. http://dx.doi.org/10.1016/j.devcel.2007.03.005

Chen, P.X., B.D. Ostrow, S.R. Tafuri, and R.L. Chisholm. 1994. Targeted disruption of the *Dictyostelium* RMLC gene produces cells defective in cytokinesis and development. *J. Cell Biol.* 127:1933–1944. http://dx.doi.org/10.1083/jcb.127.6.1933

Derivery, E., J. Fink, D. Martin, A. Houdusse, M. Piel, T.E. Stradal, D. Louvard, and A. Gautreau. 2008. Free Brick1 is a trimeric precursor in the assembly of a functional wave complex. *PLoS ONE.* 3:e2462. http://dx.doi.org/10.1371/journal.pone.0002462

Diz-Muñoz, A., M. Krieg, M. Bergert, I. Ibarlucea-Benitez, D.J. Muller, E. Paluch, and C.P. Heisenberg. 2010. Control of directed cell migration in vivo by membrane-to-cortex attachment. *PLoS Biol.* 8:e1000544. http://dx.doi.org/10.1371/journal.pbio.1000544

Dormann, D., G. Weijer, S. Dowler, and C.J. Weijer. 2004. In vivo analysis of 3-phosphoinositide dynamics during *Dictyostelium* phagocytosis and chemotaxis. *J. Cell Sci.* 117:6497–6509. http://dx.doi.org/10.1242/jcs.01579

Faix, J., L. Kreppel, G. Shaulsky, M. Schleicher, and A.R. Kimmel. 2004. A rapid and efficient method to generate multiple gene disruptions in *Dictyostelium discoideum* using a single selectable marker and the Cre-loxP system. *Nucleic Acids Res.* 32:e143. http://dx.doi.org/10.1093/nar/gnh136

Fets, L., J.M. Nichols, and R.R. Kay. 2014. A PIP5 kinase essential for efficient chemotactic signalling. *Curr. Biol.* 24:415–421. http://dx.doi.org/10.1016/j.cub.2013.12.052

Fink, R.D., and J.P. Trinkaus. 1988. Fundulus deep cells: directional migration in response to epithelial wounding. *Dev. Biol.* 129:179–190. http://dx.doi.org/10.1016/0012-1606(88)90172-8

Funamoto, S., K. Milan, R. Meili, and R.A. Firtel. 2001. Role of phosphatidylinositol 3′ kinase and a downstream pleckstrin homology domain-containing protein in controlling chemotaxis in *Dictyostelium. J. Cell Biol.* 153:795–810. http://dx.doi.org/10.1083/jcb.153.4.795

Gerald, N., J. Dai, H.P. Ting-Beall, and A. De Lozanne. 1998. A role for *Dictyostelium* racE in cortical tension and cleavage furrow progression. *J. Cell Biol.* 141:483–492. http://dx.doi.org/10.1083/jcb.141.2.483

Hall, A.L., A. Schlein, and J. Condeelis. 1988. Relationship of pseudopod extension to chemotactic hormone-induced actin polymerization in amoeboid cells. *J. Cell. Biochem.* 37:285–299. http://dx.doi.org/10.1002/jcb.240370304

Hartigan, J.A., and P.M. Hartigan. 1985. The dip test of unimodality. *Ann. Stat.* 13:70–84. http://dx.doi.org/10.1214/aos/1176346577

Haugwitz, M., A.A. Noegel, J. Karakesisoglou, and M. Schleicher. 1994. *Dictyostelium* amoebae that lack G-actin-sequestering profilins show defects in F-actin content, cytokinesis, and development. *Cell.* 79:303–314. http://dx.doi.org/10.1016/0092-8674(94)90199-6

Hitt, A.L., J.H. Hartwig, and E.J. Luna. 1994. Ponticulin is the major high affinity link between the plasma membrane and the cortical actin network in *Dictyostelium. J. Cell Biol.* 126:1433–1444. http://dx.doi.org/10.1083/jcb.126.6.1433

Hoeller, O., and R.R. Kay. 2007. Chemotaxis in the absence of PIP3 gradients. *Curr. Biol.* 17:813–817. http://dx.doi.org/10.1016/j.cub.2007.04.004

Hoeller, O., P. Bolourani, J. Clark, L.R. Stephens, P.T. Hawkins, O.D. Weiner, G. Weeks, and R.R. Kay. 2013. Two distinct functions for PI3-kinases in macropinocytosis. *J. Cell Sci.* 126:4296–4307. http://dx.doi.org/10.1242/jcs.134015

Ibarra, N., S.L. Blagg, F. Vazquez, and R.H. Insall. 2006. Nap1 regulates *Dictyostelium* cell motility and adhesion through SCAR-dependent and -independent pathways. *Curr. Biol.* 16:717–722. http://dx.doi.org/10.1016/j.cub.2006.02.068

Iijima, M., and P. Devreotes. 2002. Tumor suppressor PTEN mediates sensing of chemoattractant gradients. *Cell.* 109:599–610. http://dx.doi.org/10.1016/S0092-8674(02)00745-6

Insall, R.H. 2010. Understanding eukaryotic chemotaxis: a pseudopod-centred view. *Nat. Rev. Mol. Cell Biol.* 11:453–458. http://dx.doi.org/10.1038/nrm2905

Insall, R.H., and L.M. Machesky. 2009. Actin dynamics at the leading edge: from simple machinery to complex networks. *Dev. Cell.* 17:310–322. http://dx.doi.org/10.1016/j.devcel.2009.08.012

Insall, R., A. Kuspa, P.J. Lilly, G. Shaulsky, L.R. Levin, W.F. Loomis, and P. Devreotes. 1994. CRAC, a cytosolic protein containing a pleckstrin homology domain, is required for receptor and G protein-mediated activation of adenylyl cyclase in *Dictyostelium. J. Cell Biol.* 126:1537–1545. http://dx.doi.org/10.1083/jcb.126.6.1537

Kamimura, Y., Y. Xiong, P.A. Iglesias, O. Hoeller, P. Bolourani, and P.N. Devreotes. 2008. PIP3-independent activation of TorC2 and PKB at the cell's leading edge mediates chemotaxis. *Curr. Biol.* 18:1034–1043. http://dx.doi.org/10.1016/j.cub.2008.06.068

Kay, R.R. 1987. Cell differentiation in monolayers and the investigation of slime mold morphogens. *Methods Cell Biol.* 28:433–448. http://dx.doi.org/10.1016/S0091-679X(08)61661-1

Kay, R.R., and C.R.L. Thompson. 2009. Cold Spring Harbor Perspectives in Biology: Generation and Interpretation of Morphogen Gradients. Cold Spring Harbor Press. Cold Spring Harbor, NY.

Kay, R.R., P. Langridge, D. Traynor, and O. Hoeller. 2008. Changing directions in the study of chemotaxis. *Nat. Rev. Mol. Cell Biol.* 9:455–463.

King, J.S., and R.H. Insall. 2009. Chemotaxis: finding the way forward with *Dictyostelium. Trends Cell Biol.* 19:523–530. http://dx.doi.org/10.1016/j.tcb.2009.07.004

Knecht, D.A., and W.F. Loomis. 1988. Developmental consequences of the lack of myosin heavy chain in *Dictyostelium discoideum. Dev. Biol.* 128:178–184. http://dx.doi.org/10.1016/0012-1606(88)90280-1

Kortholt, A., J.S. King, I. Keizer-Gunnink, A.J. Harwood, and P.J. Van Haastert. 2007. Phospholipase C regulation of phosphatidylinositol 3,4,5-trisphosphate-mediated chemotaxis. *Mol. Biol. Cell.* 18:4772–4779. http://dx.doi.org/10.1091/mbc.E07-05-0407

Laevsky, G., and D.A. Knecht. 2001. Under-agarose folate chemotaxis of *Dictyostelium discoideum* amoebae in permissive and mechanically inhibited conditions. *Biotechniques*. 31:1140–1142: 1144: 1146–1149.

Lämmermann, T., and M. Sixt. 2009. Mechanical modes of 'amoeboid' cell migration. *Curr. Opin. Cell Biol.* 21:636–644. http://dx.doi.org/10.1016/j.ceb.2009.05.003

Langridge, P.D., and R.R. Kay. 2006. Blebbing of *Dictyostelium* cells in response to chemoattractant. *Exp. Cell Res.* 312:2009–2017. http://dx.doi.org/10.1016/j.yexcr.2006.03.007

Langridge, P.D., and R.R. Kay. 2007. Mutants in the *Dictyostelium* Arp2/3 complex and chemoattractant-induced actin polymerization. *Exp. Cell Res.* 313:2563–2574. http://dx.doi.org/10.1016/j.yexcr.2007.04.029

Lee, S., F.I. Comer, A. Sasaki, I.X. McLeod, Y. Duong, K. Okumura, J.R. Yates III, C.A. Parent, and R.A. Firtel. 2005. TOR complex 2 integrates cell movement during chemotaxis and signal relay in *Dictyostelium. Mol. Biol. Cell*. 16:4572–4583. http://dx.doi.org/10.1091/mbc.E05-04-0342

Maaloum, M., N. Pernodet, and B. Tinland. 1998. Agarose gel structure using atomic force microscopy: gel concentration and ionic strength effects. *Electrophoresis*. 19:1606–1610. http://dx.doi.org/10.1002/elps.1150191015

Maeda, M., H. Kuwayama, M. Yokoyama, K. Nishio, T. Morio, H. Urushihara, M. Katoh, Y. Tanaka, T. Saito, H. Ochiai, et al. 2000. Developmental changes in the spatial expression of genes involved in myosin function in *Dictyostelium. Dev. Biol.* 223:114–119. http://dx.doi.org/10.1006/dbio.2000.9736

McRobbie, S.J., and P.C. Newell. 1983. Changes in actin associated with the cytoskeleton following chemotactic stimulation of *Dictyostelium discoideum*. *Biochem. Biophys. Res. Commun.* 115:351–359. http://dx.doi.org/10.1016/0006-291X(83)91011-2

Meili, R., C. Ellsworth, S. Lee, T.B.K. Reddy, H. Ma, and R.A. Firtel. 1999. Chemoattractant-mediated transient activation and membrane localization of Akt/PKB is required for efficient chemotaxis to cAMP in *Dictyostelium. EMBO J.* 18:2092–2105. http://dx.doi.org/10.1093/emboj/18.8.2092

Mogilner, A., and G. Oster. 1996. Cell motility driven by actin polymerization. *Biophys. J.* 71:3030–3045. http://dx.doi.org/10.1016/S0006-3495(96)79496-1

Otto, A., H. Collins-Hooper, A. Patel, P.R. Dash, and K. Patel. 2011. Adult skeletal muscle stem cell migration is mediated by a blebbing/amoeboid mechanism. *Rejuvenation Res.* 14:249–260. http://dx.doi.org/10.1089/rej.2010.1151

Pang, K.M., E. Lee, and D.A. Knecht. 1998. Use of a fusion protein between GFP and an actin-binding domain to visualize transient filamentous-actin structures. *Curr. Biol.* 8:405–408. http://dx.doi.org/10.1016/S0960-9822(98)70159-9

Parent, C.A., B.J. Blacklock, W.M. Froehlich, D.B. Murphy, and P.N. Devreotes. 1998. G protein signaling events are activated at the leading edge of chemotactic cells. *Cell*. 95:81–91. http://dx.doi.org/10.1016/S0092-8674(00)81784-5

Parikh, A., E.R. Miranda, M. Katoh-Kurasawa, D. Fuller, G. Rot, L. Zagar, T. Curk, R. Sucgang, R. Chen, B. Zupan, et al. 2010. Conserved developmental transcriptomes in evolutionarily divergent species. *Genome Biol.* 11:R35. http://dx.doi.org/10.1186/gb-2010-11-3-r35

Petrie, R.J., N. Gavara, R.S. Chadwick, and K.M. Yamada. 2012. Nonpolarized signaling reveals two distinct modes of 3D cell migration. *J. Cell Biol.* 197:439–455. http://dx.doi.org/10.1083/jcb.201201124

Pitt, G.S., N. Milona, J. Borleis, K.C. Lin, R.R. Reed, and P.N. Devreotes. 1992. Structurally distinct and stage-specific adenylyl cyclase genes play different roles in *Dictyostelium* development. *Cell*. 69:305–315. http://dx.doi.org/10.1016/0092-8674(92)90411-5

Pollard, T.D., and G.G. Borisy. 2003. Cellular motility driven by assembly and disassembly of actin filaments. *Cell*. 112:453–465. http://dx.doi.org/10.1016/S0092-8674(03)00120-X

Pollitt, A.Y., S.L. Blagg, N. Ibarra, and R.H. Insall. 2006. Cell motility and SCAR localisation in axenically growing *Dictyostelium* cells. *Eur. J. Cell Biol.* 85:1091–1098. http://dx.doi.org/10.1016/j.ejcb.2006.05.014

Postma, M., and P.J. van Haastert. 2009. Mathematics of experimentally generated chemoattractant gradients. *Methods Mol. Biol.* 571:473–488. http://dx.doi.org/10.1007/978-1-60761-198-1_31

Raucher, D., T. Stauffer, W. Chen, K. Shen, S. Guo, J.D. York, M.P. Sheetz, and T. Meyer. 2000. Phosphatidylinositol 4,5-bisphosphate functions as a second messenger that regulates cytoskeleton-plasma membrane adhesion. *Cell*. 100:221–228. http://dx.doi.org/10.1016/S0092-8674(00)81560-3

Riedl, J., A.H. Crevenna, K. Kessenbrock, J.H. Yu, D. Neukirchen, M. Bista, F. Bradke, D. Jenne, T.A. Holak, Z. Werb, et al. 2008. Lifeact: a versatile marker to visualize F-actin. *Nat. Methods*. 5:605–607. http://dx.doi.org/10.1038/nmeth.1220

Sahai, E., and C.J. Marshall. 2003. Differing modes of tumour cell invasion have distinct requirements for Rho/ROCK signalling and extracellular proteolysis. *Nat. Cell Biol.* 5:711–719. http://dx.doi.org/10.1038/ncb1019

Sanz-Moreno, V., G. Gadea, J. Ahn, H. Paterson, P. Marra, S. Pinner, E. Sahai, and C.J. Marshall. 2008. Rac activation and inactivation control plasticity of tumor cell movement. *Cell*. 135:510–523. http://dx.doi.org/10.1016/j.cell.2008.09.043

Segall, J.E., A. Kuspa, G. Shaulsky, M. Ecke, M. Maeda, C. Gaskins, R.A. Firtel, and W.F. Loomis. 1995. A MAP kinase necessary for receptor-mediated activation of adenylyl cyclase in *Dictyostelium. J. Cell Biol.* 128:405–413. http://dx.doi.org/10.1083/jcb.128.3.405

Shina, M.C., A. Müller-Taubenberger, C. Unal, M. Schleicher, M. Steinert, L. Eichinger, R. Müller, R. Blau-Wasser, G. Glöckner, and A.A. Noegel. 2011. Redundant and unique roles of coronin proteins in *Dictyostelium. Cell. Mol. Life Sci.* 68:303–313. http://dx.doi.org/10.1007/s00018-010-0455-y

Silveira, L.A., J.L. Smith, J.L. Tan, and J.A. Spudich. 1998. MLCK-A, an unconventional myosin light chain kinase from *Dictyostelium*, is activated by a cGMP-dependent pathway. *Proc. Natl. Acad. Sci. USA*. 95:13000–13005. http://dx.doi.org/10.1073/pnas.95.22.13000

Suraneni, P., B. Rubinstein, J.R. Unruh, M. Durnin, D. Hanein, and R. Li. 2012. The Arp2/3 complex is required for lamellipodia extension and directional fibroblast cell migration. *J. Cell Biol.* 197:239–251. http://dx.doi.org/10.1083/jcb.201112113

Svitkina, T.M., and G.G. Borisy. 1999. Arp2/3 complex and actin depolymerizing factor/cofilin in dendritic organization and treadmilling of actin filament array in lamellipodia. *J. Cell Biol.* 145:1009–1026. http://dx.doi.org/10.1083/jcb.145.5.1009

Swaney, K.F., C.H. Huang, and P.N. Devreotes. 2010. Eukaryotic chemotaxis: a network of signaling pathways controls motility, directional sensing, and polarity. *Annu Rev Biophys*. 39:265–289. http://dx.doi.org/10.1146/annurev.biophys.093008.131228

Swanson, J.A., and D.L. Taylor. 1982. Local and spatially coordinated movements in *Dictyostelium discoideum* amoebae during chemotaxis. *Cell*. 28:225–232. http://dx.doi.org/10.1016/0092-8674(82)90340-3

Tinevez, J.Y., U. Schulze, G. Salbreux, J. Roensch, J.F. Joanny, and E. Paluch. 2009. Role of cortical tension in bleb growth. *Proc. Natl. Acad. Sci. USA*. 106:18581–18586. http://dx.doi.org/10.1073/pnas.0903353106

Tozluoğlu, M., A.L. Tournier, R.P. Jenkins, S. Hooper, P.A. Bates, and E. Sahai. 2013. Matrix geometry determines optimal cancer cell migration strategy and modulates response to interventions. *Nat. Cell Biol.* 15:751–762. http://dx.doi.org/10.1038/ncb2775

Traynor, D., and R.R. Kay. 2007. Possible roles of the endocytic cycle in cell motility. *J. Cell Sci.* 120:2318–2327. http://dx.doi.org/10.1242/jcs.007732

Traynor, D., J.L. Milne, R.H. Insall, and R.R. Kay. 2000. Ca(2+) signalling is not required for chemotaxis in *Dictyostelium. EMBO J.* 19:4846–4854. http://dx.doi.org/10.1093/emboj/19.17.4846

Trinkaus, J.P. 1973. Surface activity and locomotion of Fundulus deep cells during blastula and gastrula stages. *Dev. Biol.* 30:69–103. http://dx.doi.org/10.1016/0012-1606(73)90049-3

Trinkaus, J.P., M. Trinkaus, and R.D. Fink. 1992. On the convergent cell movements of gastrulation in *Fundulus*. *J. Exp. Zool.* 261:40–61. http://dx.doi.org/10.1002/jez.1402610107

Tsujioka, M., L.M. Machesky, S.L. Cole, K. Yahata, and K. Inouye. 1999. A unique talin homologue with a villin headpiece-like domain is required for multicellular morphogenesis in *Dictyostelium. Curr. Biol.* 9:389–392. http://dx.doi.org/10.1016/S0960-9822(99)80169-9

Tsujioka, M., K. Yoshida, A. Nagasaki, S. Yonemura, A. Müller-Taubenberger, and T.Q. Uyeda. 2008. Overlapping functions of the two talin homologues in *Dictyostelium. Eukaryot. Cell*. 7:906–916. http://dx.doi.org/10.1128/EC.00464-07

Tyson, R.A., D.B.A. Epstein, K.I. Anderson, and T. Bretschneider. 2010. High resolution tracking of cell membrane dynamics in moving cells: an electrifying approach. *Math. Model. Nat. Phenom.* 5:34–55. http://dx.doi.org/10.1051/mmnp/20105102

Veltman, D.M., G. Akar, L. Bosgraaf, and P.J. Van Haastert. 2009. A new set of small, extrachromosomal expression vectors for *Dictyostelium discoideum*. *Plasmid*. 61:110–118. http://dx.doi.org/10.1016/j.plasmid.2008.11.003

Wang, B., G. Shaulsky, and A. Kuspa. 1999. Multiple developmental roles for CRAC, a cytosolic regulator of adenylyl cyclase. *Dev. Biol.* 208:1–13. http://dx.doi.org/10.1006/dbio.1998.9193

Wolf, K., I. Mazo, H. Leung, K. Engelke, U.H. von Andrian, E.I. Deryugina, A.Y. Strongin, E.B. Bröcker, and P. Friedl. 2003. Compensation mechanism in tumor cell migration: mesenchymal-amoeboid transition after blocking of pericellular proteolysis. *J. Cell Biol.* 160:267–277. http://dx.doi.org/10.1083/jcb.200209006

Wolf, K., M. Te Lindert, M. Krause, S. Alexander, J. Te Riet, A.L. Willis, R.M. Hoffman, C.G. Figdor, S.J. Weiss, and P. Friedl. 2013. Physical limits of cell migration: control by ECM space and nuclear deformation and tuning by proteolysis and traction force. *J. Cell Biol.* 201:1069–1084. http://dx.doi.org/10.1083/jcb.201210152

Wu, C., S.B. Asokan, M.E. Berginski, E.M. Haynes, N.E. Sharpless, J.D. Griffith, S.M. Gomez, and J.E. Bear. 2012. Arp2/3 is critical for lamellipodia and response to extracellular matrix cues but is dispensable for chemotaxis. *Cell*. 148:973–987. http://dx.doi.org/10.1016/j.cell.2011.12.034

Wu, L.J., R. Valkema, P.J.M. Van Haastert, and P.N. Devreotes. 1995. The G protein beta subunit is essential for multiple responses to chemoattractants in *Dictyostelium*. *J. Cell Biol.* 129:1667–1675. http://dx.doi.org/10.1083/jcb.129.6.1667

Xiao, Z., N. Zhang, D.B. Murphy, and P.N. Devreotes. 1997. Dynamic distribution of chemoattractant receptors in living cells during chemotaxis and persistent stimulation. *J. Cell Biol.* 139:365–374. http://dx.doi.org/10.1083/jcb.139.2.365

Xiong, Y., C.H. Huang, P.A. Iglesias, and P.N. Devreotes. 2010. Cells navigate with a local-excitation, global-inhibition-biased excitable network. *Proc. Natl. Acad. Sci. USA*. 107:17079–17086. http://dx.doi.org/10.1073/pnas.1011271107

Yoshida, K., and K. Inouye. 2001. Myosin II-dependent cylindrical protrusions induced by quinine in *Dictyostelium*: antagonizing effects of actin polymerization at the leading edge. *J. Cell Sci.* 114:2155–2165.

Yoshida, K., and T. Soldati. 2006. Dissection of amoeboid movement into two mechanically distinct modes. *J. Cell Sci.* 119:3833–3844. http://dx.doi.org/10.1242/jcs.03152